J|A|C|S
ARTICLES

Published on Web 02/10/2009

# Adaptation to Shape Switching by Component Selection in a Constitutional Dynamic System

Sébastien Ulrich and Jean-Marie Lehn*

*Institut de Science et d'Ingénierie Supramoléculaires (ISIS), 8 allée Gaspard Monge, 67083 Strasbourg, France*

Received December 17, 2008; E-mail: lehn@isis.u-strasbg.fr

***Abstract:*** Molecules having different accessible shape states, which can be addressed in an effector-controlled manner, may be termed morphological switches. A dynamic covalent system can undergo adaptation to each state of a two-state morphological switch by generation of an optimal constitution through component selection. We have studied such a component selection in the dynamic covalent constituents generated by metal cation-induced shape switching of a core component between two states of W and U shape, characterized by both different geometries and different coordination features. The system performs shape-dependent self-sorting of metal ions and components. The origin of the selectivity was investigated through competition experiments, in solution and by analysis of solid state structures, which reveal the role of the molecular shape in the formation of a particular self-assembled architecture. The coordination features of each state as well as phase change also play an important role, in addition to the shape plasticity, in steering the covalent dynamic system toward the formation of a given entity by the selection of the most appropriate components. Different examples are described which show that the morphological switching of one component of a given self-assembled entity can lead to the exchange of the complementary one, which is no longer the best partner, for a new partner, able to form a more stable new assembly. Thus, the constitutional evolution of these dynamic systems is steered by the shape of a given state via both its geometry and its coordination features toward metal ions, leading to incorporation/decorporation of the most appropriate components. The controlled interconversion of the shape states of the morphological switches, induced by addition/removal of metal ions, results in a constitutional adaptation behavior through inversion of the selection preferences.

## 1. Introduction

Self-organization processes[1,2] are at the origin of the properties/functions expressed in matter. From synthetic material chemistry, e.g., the organization of liquid crystals,[3] to biological processes and eventually to the study of the origin and evolution of life,[4] it underlies every step involving the complexification of matter.[1,2,4−8] They extend in both space and time and at all scales from the molecule to the cell and eventually to living organisms. Supramolecular chemistry[9] has stressed the fact that chemistry is also a science of information and that the precise control of molecular information can lead to well-defined supramolecular self-organized entities.[10] Understanding such a correlation between molecular information and the resulting self-assembled supramolecular architecture has led to the design of many different molecular components capable of transferring their molecular information, through a particular read-out algorithm,[10−12] into the formation of well-defined architectures such as multistranded helicates,[13−17] circular helicates,[15,18] grid-like arrays,[19] rosettes,[20−22] and many others.[23−29] As noncovalent interactions, for instance, hydrogen bonds, $\pi-\pi$ stacking,

(1) (a) Lehn, J.-M. *Proc. Natl. Acad. Sci. U.S.A.* **2002**, *99*, 4763–4768. (b) In the present context, the terms "evolution" and "evolve" are used in the meaning of "change into", as in prebiotic chemical evolution. It has been pointed out in ref 1a (p 4767) and by a referee that one may consider that evolution supposes heritable information/features as in biological evolution.
(2) Lehn, J.-M. *Science* **2002**, *295*, 2400–2403.
(3) Kato, T.; Mizoshita, N.; Kishimoto, K. *Angew. Chem., Int. Ed.* **2006**, *45*, 38–68.
(4) (a) Eigen, M. *Naturwissenschaften* **1971**, *58*, 465–523. (b) Rasmussen, S.; Chen, L. H.; Deamer, D.; Krakauer, D. C.; Packard, N. H.; Stadler, P. F.; Bedau, M. A. *Science* **2004**, *303*, 963–965.
(5) Ball, P. *Nature* **2006**, *442*, 500–502.
(6) Whitesides, G. M.; Grzybowski, B. *Science* **2002**, *295*, 2418–2421.
(7) Whitesides, G. M.; Boncheva, M. *Proc. Natl. Acad. Sci. U.S.A.* **2002**, *99*, 4769–4774.
(8) Philp, D.; Stoddart, J. F. *Angew. Chem., Int. Ed. Engl.* **1996**, *35*, 1154–1196.
(9) Lehn, J.-M. *Supramolecular Chemistry*; Wiley-VCH: Weinheim, 1995.
(10) Lehn, J.-M. *Chem.—Eur. J.* **2000**, *6*, 2097–2102.
(11) Funeriu, D. P.; Rissanen, K.; Lehn, J.-M. *Proc. Natl. Acad. Sci. U.S.A.* **2001**, *98*, 10546–10551.
(12) Funeriu, D. P.; Lehn, J.-M.; Fromm, K. M.; Fenske, D. *Chem.—Eur. J.* **2000**, *6*, 2103–2111.
(13) Albrecht, M. *Angew. Chem., Int. Ed.* **2005**, *44*, 6448–6451.
(14) Lehn, J.-M.; Marquis-Rigault, A.; Siegel, J.; Harrowfield, J. M.; Chevrier, B.; Moras, D. *Proc. Natl. Acad. Sci. U.S.A.* **1987**, *84*, 2565.
(15) Albrecht, M. *Chem. Rev.* **2001**, *101*, 3457–3497.
(16) Marquis, A.; Smith, V.; Harrowfield, J.; Lehn, J.-M.; Herschbach, H.; Sanvito, R.; Leize-Wagner, E.; Van Dorsselaer, A. *Chem.—Eur. J.* **2006**, *12*, 5632–5641.
(17) Piguet, C.; Bernardinelli, G.; Hopfgartner, G. *Chem. Rev.* **1997**, *97*, 2005–2062.
(18) Hasenknopf, B.; Lehn, J.-M.; Kneisel, B. O.; Baum, G.; Fenske, D. *Angew. Chem., Int. Ed. Engl.* **1996**, *35*, 1838–1840.
(19) Ruben, M.; Rojo, J.; Romero-Salguero, F. J.; Uppadine, L. H.; Lehn, J.-M. *Angew. Chem., Int. Ed.* **2004**, *43*, 3644–3662.


**10.1021/ja809828g CCC: $40.75** 

electrostatic, or van der Waals interactions, are labile, the resulting self-assembled supramolecular object inherently displays a dynamic behavior in its constitution.[1,2,30−32] Such dynamic assemblies could display, in principle, adaptive behavior in response to different stimuli. Thus, Constitutional Dynamic Chemistry (CDC)[31,32] has evolved from implementing the dynamic behavior of assemblies, based on supramolecular interactions,[9] and to extending it also to molecular entities through incorporation of dynamic covalent bonds.[31−34] It uses the chemical diversity provided by a dynamic library to study the chemical evolution[1b] of systems, in particular in response to environmental triggers. Therefore, beyond self-organization by design, self-organization with selection thrives to investigate the evolution[1b] of competing species toward the most appropriate constitution by selection of the appropriate component. Specific structural requirements may result in the self-sorting of a dynamic library with selection of a particular component into the final architecture.[35−43] In addition to internal parameters, different external factors such as the template effect,[44−56] medium effect,[27,57−62] concentration,[62−64] phase change (gel formation,[65] crystallization[45,66−71]), the presence of an electric field,[72] and the hydrostatic pressure[73] have been shown to affect the constitution of dynamic systems through modification of selection preferences.

We were interested in using molecular morphology as trigger for constitutional selection, since the shape of molecules is a crucial parameter in a self-assembly process. Shape can modulate recognition events,[74−76] as illustrated by the lock-and-key principle,[77] whereas, conversely, recognition events can affect molecular shape in an induced-fit fashion.[78,79] We previously described systems that involved the design of morphological switches as core components, whose shape could be switched between a W and U shape by metal ion binding, causing the interconversion of a dynamic covalent system between polymeric and macrocyclic self-assemblies.[80,81] We


(20) Timmerman, P.; Vreekamp, R. H.; Hulst, R.; Verboom, W.; Reinhoudt, D. N.; Rissanen, K.; Udachin, K. A.; Ripmeester, J. *Chem.—Eur. J.* **1997**, *3*, 1823–1832.
(21) Whitesides, G. M.; Simanek, E. E.; Mathias, J. P.; Seto, C. T.; Chin, D. N.; Mammen, M.; Gordon, D. M. *Acc. Chem. Res.* **1995**, *28*, 37–44.
(22) Zerkowski, J. A.; Seto, C. T.; Whitesides, G. M. *J. Am. Chem. Soc.* **1992**, *114*, 5473–5475.
(23) (a) Stang, P. J.; Olenyuk, B. *Acc. Chem. Res.* **1997**, *30*, 502–518. (b) Seidel, S. R.; Stang, P. J. *Acc. Chem. Res.* **2002**, *35*, 972–983. (c) Northrop, B. H.; Yang, H-B; Stang, P. *Chem. Commun.* **2008**, 5896–5908.
(24) Greig, L. M.; Philp, D. *Chem. Soc. Rev.* **2001**, *30*, 287–302.
(25) Leininger, S.; Olenyuk, B.; Stang, P. J. *Chem. Rev.* **2000**, *100*, 853–907.
(26) Caulder, D. L.; Raymond, K. N. *Acc. Chem. Res.* **1999**, *32*, 975–982.
(27) Fujita, M. *Acc. Chem. Res.* **1999**, *32*, 53–61.
(28) Fujita, M. *Chem. Soc. Rev.* **1998**, *27*, 417–425.
(29) Saalfrank, R. W.; Maid, H.; Scheurer, A. *Angew Chem., Int. Ed.* **2008**, *47*, 8794–8824.
(30) Davis, A. V.; Yeh, R. M.; Raymond, K. N. *Proc. Natl. Acad. Sci. U.S.A.* **2002**, *99*, 4793–4796.
(31) Lehn, J.-M. *Chem. Soc. Rev.* **2007**, *36*, 151–160.
(32) Lehn, J.-M. *Chem.—Eur. J.* **1999**, *5*, 2455–2463.
(33) Rowan, S. J.; Cantrill, S. J.; Cousins, G. R. L.; Sanders, J. K. M.; Stoddart, J. F. *Angew. Chem., Int. Ed.* **2002**, *41*, 898–952.
(34) Corbett, P. T.; Leclaire, J.; Vial, L.; West, K. R.; Wietor, J. L.; Sanders, J. K. M.; Otto, S. *Chem. Rev.* **2006**, *106*, 3652–3711.
(35) Krämer, R.; Lehn, J.-M.; Marquis-Rigault, A. *Proc. Natl. Acad. Sci. U.S.A.* **1993**, *90*, 5394–5398.
(36) Nitschke, J. R.; Lehn, J.-M. *Proc. Natl. Acad. Sci. U.S.A.* **2003**, *100*, 11970–11974.
(37) Saur, B.; Scopelliti, R.; Severin, K. *Chem.—Eur. J.* **2006**, *12*, 1058–1066.
(38) Yang, H. B.; Ghosh, K.; Northrop, B. H.; Stang, P. J. *Org. Lett.* **2007**, *9*, 1561–1564.
(39) (a) Nitschke, J. R. *Acc. Chem. Res.* **2007**, *40*, 103–112. (b) Sarma, R. J.; Nitschke, J. R. *Angew. Chem., Int. Ed.* **2008**, *47*, 377–380.
(40) Legrand, Y. M.; Van der Lee, A.; Barboiu, M. *Inorg. Chem.* **2007**, *46*, 9540–9547.
(41) Zheng, Y. R.; Yang, H. B.; Northrop, B. H.; Ghosh, K.; Stang, P. J. *Inorg. Chem.* **2008**, *47*, 4706–4711.
(42) Barrett, E. S.; Dale, T. J.; Rebek, J. *J. Am. Chem. Soc.* **2008**, *130*, 2344–2350.
(43) Wu, A.; Isaacs, L *J. Am. Chem. Soc.* **2003**, *125*, 4831–4835.
(44) Kerckhoffs, J. M. C. A.; Mateos-Timoneda, M. A.; Reinhoudt, D. N.; Crego-Calama, M. *Chem.—Eur. J.* **2007**, *13*, 2377–2385.
(45) Haussmann, P. C.; Khan, S. I.; Stoddart, J. F. *J. Org. Chem.* **2007**, *72*, 6708–6713.
(46) Vial, L.; Ludlow, R. F.; Leclaire, J.; Perez-Fernandez, R.; Otto, S. *J. Am. Chem. Soc.* **2006**, *128*, 10253–10257.
(47) Sreenivasachary, N.; Hickman, D. T.; Sarazin, D.; Lehn, J.-M. *Chem.—Eur. J.* **2006**, *12*, 8581–8588.
(48) Busch, D. H. *Templates in Chemistry II*; 2005; Vol. 249.
(49) Kubota, Y.; Sakamoto, S.; Yamaguchi, K.; Fujita, M. *Proc. Natl. Acad. Sci. U.S.A.* **2002**, *99*, 4854–4856.
(50) Ramstrom, O.; Lehn, J.-M. *Nat. Rev. Drug Discovery* **2002**, *1*, 26–36.
(51) Storm, O.; Luning, U. *Chem.—Eur. J.* **2002**, *8*, 793–798.
(52) Bunyapaiboonsri, T.; Ramstrom, O.; Lohmann, S.; Lehn, J.-M.; Peng, L.; Goeldner, M. *ChemBioChem* **2001**, *2*, 438–444.
(53) Ramstrom, O.; Lehn, J.-M. *ChemBioChem* **2000**, *1*, 41–48.
(54) Hiraoka, S.; Kubota, Y.; Fujita, M. *Chem. Commun.* **2000**, 1509–1510.
(55) Hasenknopf, B.; Lehn, J.-M.; Boumediene, N.; DupontGervais, A.; VanDorsselaer, A.; Kneisel, B.; Fenske, D. *J. Am. Chem. Soc.* **1997**, *119*, 10956–10962.
(56) Nelson, S. M. *Pure Appl. Chem.* **1980**, *52*, 2461–2476.
(57) Heo, J.; Jeon, Y. M.; Mirkin, C. A. *J. Am. Chem. Soc.* **2007**, *129*, 7712–7713.
(58) Ramirez, J.; Stadler, A. M.; Kyritsakas, N.; Lehn, J.-M. *Chem. Commun.* **2007**, 237–239.
(59) Schweiger, M.; Seidel, S. R.; Arif, A. M.; Stang, P. J. *Inorg. Chem.* **2002**, *41*, 2556–2559.
(60) Oh, K.; Jeong, K. S.; Moore, J. S. *Nature* **2001**, *414*, 889–893.
(61) Baxter, P. N. W.; Lehn, J.-M.; Baum, G.; Fenske, D. *Chem.—Eur. J.* **2000**, *6*, 4510–4517.
(62) Baxter, P. N. W.; Khoury, R. G.; Lehn, J.-M.; Baum, G.; Fenske, D. *Chem.—Eur. J.* **2000**, *6*, 4140–4148.
(63) Kraus, T.; Budesinsky, M.; Cvacka, J. C.; Sauvage, J. P. *Angew. Chem., Int. Ed.* **2006**, *45*, 258–261.
(64) Kidd, T. J.; Leigh, D. A.; Wilson, A. J. *J. Am. Chem. Soc.* **1999**, *121*, 1599–1600.
(65) Sreenivasachary, N.; Lehn, J.-M. *Proc. Natl. Acad. Sci. U.S.A.* **2005**, *102*, 5938–5943.
(66) Angelin, M.; Fischer, A.; Ramstrom, O. *J. Org. Chem.* **2008**, *73*, 3593–3595.
(67) Chow, C. F.; Fujii, S.; Lehn, J.-M. *Chem. Commun.* **2007**, 4363–4365.
(68) Iwasawa, N.; Takahagi, H. *J. Am. Chem. Soc.* **2007**, *129*, 7754.
(69) Hutin, M.; Cramer, C. J.; Gagliardi, L.; Shahi, A. R. M.; Bernardinelli, G.; Cerny, R.; Nitschke, J. R. *J. Am. Chem. Soc.* **2007**, *129*, 8774–8780.
(70) Pentecost, C. D.; Chichak, K. S.; Peters, A. J.; Cave, G. W. V.; Cantrill, S. J.; Stoddart, J. F. *Angew. Chem., Int. Ed.* **2007**, *46*, 218–222.
(71) Dumitru, F.; Petit, E.; van der Lee, A.; Barboiu, M. *Eur. J. Inorg. Chem.* **2005**, 4255–4262.
(72) Giuseppone, N.; Lehn, J.-M. *Angew. Chem., Int. Ed.* **2006**, *45*, 4619–4624.
(73) Zhu, A.; Mio, M. J.; Moore, J. S.; Drickamer, H. G. *J. Phys. Chem. B* **2001**, *105*, 3300–3305.
(74) Eliseev, A. V.; Nelen, M. I. *Chem.—Eur. J.* **1998**, *4*, 825–834.
(75) Eliseev, A. V.; Nelen, M. I. *J. Am. Chem. Soc.* **1997**, *119*, 1147–1148.
(76) Fiedler, D.; Leung, D. H.; Bergman, R. G.; Raymond, K. N. *Acc. Chem. Res.* **2005**, *38*, 349–358.
(77) Fischer, E. *Ber. Dtsch. Chem. Ges.* **1894**, *27*, 2985–2993.
(78) Berl, V.; Krische, M. J.; Huc, I.; Lehn, J.-M.; Schmutz, M. *Chem.—Eur. J.* **2000**, *6*, 1938–1946.
(79) Berl, V.; Huc, I.; Lehn, J.-M.; DeCian, A.; Fischer, J. *Eur. J. Org. Chem.* **1999**, 3089–3094.
(80) Ulrich, S.; Lehn, J.-M. *Angew. Chem., Int. Ed.* **2008**, *47*, 2240–2243.

***Scheme 1.*** Constitutional Adaptation Induced by Molecular Shape Changes[a]

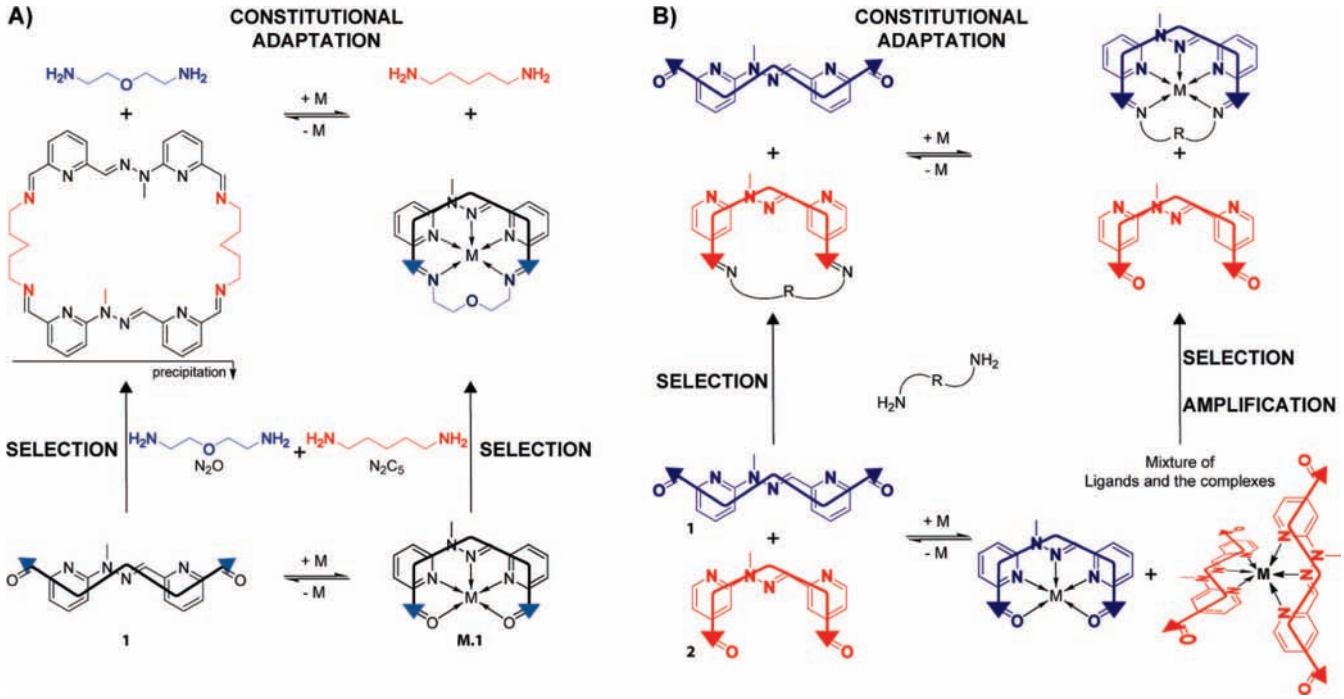


[a] (A) A particular diamine is selected from a mixture due to phase separation (left) and intrinsic preference of the U-shaped metal complex (right). The switching of the dialdehyde shape between W and U shapes induces the adaptation, i.e., the change in the selection of a component. (B) A single diamine self-assembles selectively with the most appropriate dialdehyde, while the shape-switching of that mixture of dialdehydes results in the opposite selection preference. "M" = Pb(II). Note that using the diamine $\mathbf{N_2C_5}$ generates the [1 + 1] macrocycle as depicted at the top left, whereas the use of $\mathbf{N_2O}$ generates the [2 + 2] macrocycle (see text).

now report that the morphological information borne by these switching units can be translated into the constitution of the assemblies by a dynamic covalent self-assembly process, through component selection. Thus the morphological switching process results in a constitutional adaptation behavior (Scheme 1).

## 2. Results and Discussion

**2.1. Structural Features and Shape Switching of the Morphological Switches.** Morphological switches may be defined as molecules of well-defined shape which can be converted into one or several other states of well-defined shape in an effector-controlled manner. Based on theoretical models[82] and previous experimental studies,[83−87] we chose to use the pyridine−hydrazone−pyridine scaffold, a structure isomorphic of the well-known 2,2′:6′,2″-terpyridine,[88] but synthetically much more easily accessible,[89] whose shape can be switched by metal ion binding (Scheme 2).

These morphological switches were appended with aldehyde groups to connect them to their surroundings through the formation of reversible covalent imine bonds.[33,90] In this way, it would become possible to study the relationship between the shape state and the entities generated by covalent connection with a surrounding mixture of reactive partners such as diamines.

Ligand **1** adopts a W shape in its uncomplexed state, which can be switched to a U shape on metal ion binding. These shapes and the related shape switching process were studied in the solid state by X-ray crystallography and in solution by NMR spectroscopy.[81] In addition to the previously reported examples of the use of zinc(II) and lead(II),[81] we also make here use of mercury(II) to trigger the shape switching of ligand **1** from a W to U shape. $^1$H NMR titration of **1** by mercury triflate provides evidence of the formation of the corresponding ML-type (M: metal ion, L: ligand) complex, by showing that a new species is quantitatively formed after addition of 1.0 equiv of metal ion (Supporting Information).

COSY and ROESY 2D NMR confirmed that a shape-switching process had occurred on binding of a mercury ion (Supporting Information). X-ray diffraction analysis showed that **Hg.1** has indeed the U-shaped structure depicted in Figure 1 in the solid state (Figure 1). Coordination of a mercury ion is provided by the three nitrogens and the two aldehyde oxygens from the ligand, which are almost coplanar. The two counteranions complete the coordination sphere by binding to the metal ion in the axial positions of a distorted pentagonal bipyramid.

High-resolution mass spectroscopy confirms that **Hg.1** is also the product formed in the solution state after 1.0 equiv of mercury triflate has been added to **1** (Supporting Information). An important feature of ligand **1** is that it can adapt its U-shape to the size of the central metal ion. One can then,

(81) Ulrich, S. ; Buhler, E. ; Lehn, J.-M. *New J. Chem.* **2009**, DOI 10.1039/b817261g.
(82) Howard, S. T. *J. Am. Chem. Soc.* **1996**, *118*, 10269–10274.
(83) Barboiu, M.; Lehn, J.-M. *Proc. Natl. Acad. Sci. U.S.A.* **2002**, *99*, 5201–5206.
(84) Stadler, A. M.; Kyritsakas, N.; Graff, R.; Lehn, J.-M. *Chem.—Eur. J.* **2006**, *12*, 4503–4522.
(85) Stadler, A. M.; Kyritsakas, N.; Lehn, J.-M. *Chem. Commun.* **2004**, 2024–2025.
(86) Petitjean, A.; Khoury, R. G.; Kyritsakas, N.; Lehn, J.-M. *J. Am. Chem. Soc.* **2004**, *126*, 6637–6647.
(87) Ulrich, S.; Lehn, J.-M., Unpublished results.
(88) Constable, E. C. *Chem. Soc. Rev.* **2007**, *36*, 246–253.
(89) Gardinier, K. M.; Khoury, R. G.; Lehn, J.-M. *Chem.—Eur. J.* **2000**, *6*, 4124–4131.
(90) Meyer, C. D.; Joiner, C. S.; Stoddart, J. F. *Chem. Soc. Rev.* **2007**, *36*, 1705–1723.

***Scheme 2.*** Morphological Switches **1** and **2** and Their Related W−U Shape Switching Processes Triggered by Metal Ions[a]

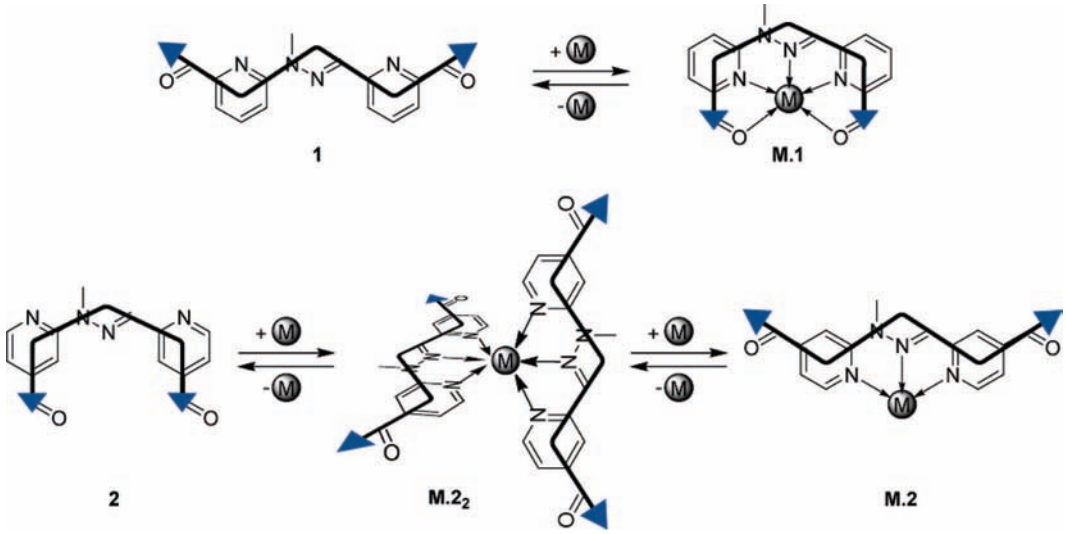


[a] "+M" refers to the addition of a metal salt, whereas "−M" refers to the addition of a competing better metal ion binder.

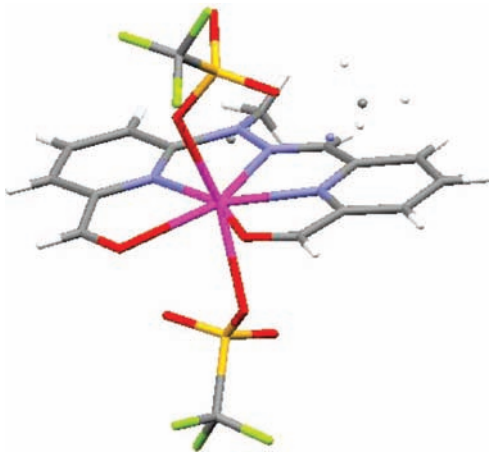

***Figure 1.*** Solid state structure of **Hg.1** obtained from X-ray diffraction analysis and revealing the U-shaped state.

from the solid state structures, measure the pinching angle and the characteristic distance between the two carbons of the two aldehyde groups (Figure 2). Such a fine geometrical tuning feature is expected to have an influence on the reaction with diamines (see below).

As expected pinching is maximum in the case of the smallest metal ion. The case of lead is peculiar since in this case the coordination number is 8 and not 7, as for zinc and mercury, due to the presence of an extra coordinating triflate molecule. This fact explains why the difference of pinching angle between lead and mercury is much higher than between mercury and zinc (the same holds for the distance d), compared to the difference of ionic radius between these ions.

The characterization of the U-shaped structure of **2** and the shape switching processes induced by metal ion (zinc(II) and lead(II)) has been recently reported.[81] While the U-shaped complexes **M.1** have a very well-defined structure both in solution and in the solid state, due to metal ion coordination in particular to the oxygens of the aldehyde groups, the U-shaped molecule **2** has a much more flexible structure since the aldehyde groups can freely rotate around the carbon−carbon bonds.

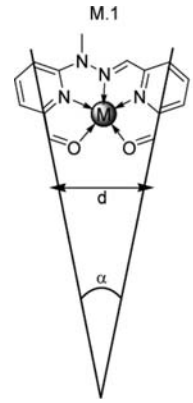


| Metal ion | Ionic radius (Å) | Pinching angle (α) (°) | Distance d (Å) |
|---|---|---|---|
| Zn (II) | 0.82 | 28.5 | 5.15 |
| Hg (II) | 1.08 | 22.8 | 5.57 |
| Pb (II) | 1.29 | 9.1 | 6.46 |

***Figure 2.*** Structural characteristics (pinching angle α and distance *d* measured in the solid state structure obtained from X-ray crystallography) showing the adaptive wrapping of ligand **1** to the size of metal ions.[91] In all cases, the counteranions used were triflates.

**2.2. Component Selection in Covalent Dynamic Self-Assembly Processes of M.1.** The presence of aldehyde groups in **1** and **2** allows for the investigation of selection processes in the generation of shape-state-dependent constitutional partners through dynamic covalent reaction with diamines. Different parameters may contribute to such a selection, in particular, geometrical, coordination, and metal ion features.

Since the U-shaped metal complexes have a well-defined shape (see above), one might expect that diamines of a length fitting best with the distance between the aldehyde groups and/or whose structure leads to the most stable product could be selected from a mixture of diamines, to form the corresponding [1 + 1] metallo-macrocycles (Scheme 3); both kinetic[92] and thermodynamic selection may take place.

Mixtures of alkyl diamines of different length (Figure 3) were thus chosen to study whether a geometrical selection is induced by the morphological information borne by the structure of **M.1**.

**2.2.1. Metal Ion-Dependent Geometrical Selection of Diamines: Case of Zn.1.** In a typical experiment, 1 equiv of the metal ion was added to a mixture of **1** and two different diamines in $CDCl_3/CD_3CN$ mixtures at 5 mM concentration and the

(91) The reported ionic radii were obtained from the *Handbook of Chemistry and Physics*, 82th ed.

(92) Nguyen, R.; Huc, I. *Angew. Chem., Int. Ed.* **2001**, *40*, 1774–1776.

***Scheme 3.*** Representation of the Selection Process Operated by the U-Shaped Metal Complex between Two Different Diamines through a Dynamic Covalent Self-Assembly

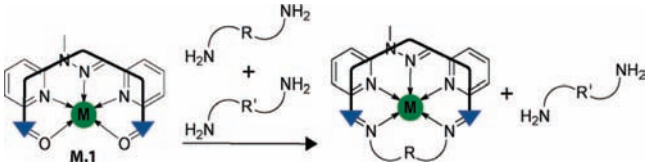


reaction was monitored until equilibrium was reached. The analyses of the composition of the solutions and the identification of the products formed by proton NMR and mass spectrometry were conducted directly on the reaction mixture so as to preserve the equilibrium conditions. As a consequence, broadening of the proton NMR signals may occur, due to exchange processes and/or interactions between the compounds present, as indicated by control experiments (see below).

All diamines from $\mathbf{N_2C_2}$ to $\mathbf{N_2C_5}$ reacted with **Zn.1** to give quantitatively the corresponding diimine metallo-macrocycle. Whereas the condensation of $\mathbf{N_2C_4}$ and $\mathbf{N_2C_5}$ proceeded smoothly at room temperature, the reaction of $\mathbf{N_2C_2}$ and $\mathbf{N_2C_3}$ required extensive heating to yield a quantitative formation of the product. This behavior could be due to the fact that short diamines can form cyclic aminal products as kinetic intermediates, which rearrange slowly into the cyclic diimine thermodynamic products.[56] The molecular structures of the macrocycles obtained were demonstrated by combining $^1$H NMR spectroscopy (and additional COSY-ROESY 2D NMR spectroscopy in some cases, see Supporting Information), which shows the imine proton peaks, MALDI-TOF mass spectrometry (Supporting Information), and single crystal X-ray diffraction. Full characterizations, including the solid state structure, were previously reported for $\mathbf{Zn.1.N_2C_4}$ and $\mathbf{Zn.1.N_2C_5}$.[81] We report here the solid state structure of $\mathbf{Zn.1.N_2C_2}$ and $\mathbf{Zn.1.N_2C_3}$. For $\mathbf{Zn.1.N_2C_2}$, crystals of the monohemiaminal of the macrocycle were obtained, whereas, for $\mathbf{Zn.1.N_2C_3}$, the structure was that of the diimine (Figure 4).[93] Whereas the diimine $\mathbf{Zn.1.N_2C_2}$ has been clearly identified as the product resulting from the reaction between the diamine and the U-shaped metal complex in solution, an intense peak corresponding to a monohemiaminal, alongside a smaller peak corresponding to a bis-hemiaminal, was also observed by MALDI-TOF mass spectrometry.

The coordination of the central metal ion is provided by five nitrogen atoms, which are almost coplanar. The additional sites in the axial positions of the pentagonal bipyramid are occupied by one counteranion and one water molecule.

Competition experiments performed in solution between $\mathbf{N_2C_2}$, $\mathbf{N_2C_3}$, or $\mathbf{N_2C_4}$ and $\mathbf{N_2C_5}$ showed in all three cases the selective formation of the smaller macrocycle as the thermodynamic product, respectively, $\mathbf{Zn.1.N_2C_2}$, $\mathbf{Zn.1.N_2C_3}$, and $\mathbf{Zn.1.N_2C_4}$. A representative case, the competition between $\mathbf{N_2C_4}$ and $\mathbf{N_2C_5}$, is depicted in Figure 5 (see Supporting Information for others).

Even though the NMR spectra of both macrocycles are very similar, as expected due to their structural resemblance, the peak corresponding to the C*H* of the central hydrazone is characteristic (7.99 ppm in $\mathbf{Zn.1.N_2C_4}$ and ca. 8.06 ppm in $\mathbf{Zn.1.N_2C_5}$) and therefore allows us to conclude that the shorter $\mathbf{N_2C_4}$ diamine has been selected at the expense of the longer $\mathbf{N_2C_5}$, showing that a difference of a single carbon in the chain is sufficient for a complete selection, corresponding to an energy difference between the two macrocycles higher than 2 kcal·mol$^{-1}$. This reflects that **Zn.1** has a well-defined U shape which imposes a geometrical selection when different diamines are in competition. In line with the conditions required to form the macrocycles (see above), the competition experiment performed with the short diamines $\mathbf{N_2C_2}$ and $\mathbf{N_2C_3}$ required extensive heating to reach thermodynamic equilibrium, whereas that between $\mathbf{N_2C_4}$ and $\mathbf{N_2C_5}$ was performed at room temperature. To fully investigate the energetic profiles of those macrocycles, competition experiments were also performed between $\mathbf{N_2C_2}$ and $\mathbf{N_2C_4}$ and between $\mathbf{N_2C_3}$ and $\mathbf{N_2C_4}$. The former showed, by $^1$H NMR, a mixture of both macrocycles in ratios of 65% of $\mathbf{Zn.1.N_2C_4}$ and 35% of $\mathbf{Zn.1.N_2C_2}$, while the latter gave a mixture of 77% of $\mathbf{Zn.1.N_2C_3}$ and 23% of $\mathbf{Zn.1.N_2C_4}$ (Supporting Information). These data show that, in this series, $\mathbf{Zn.1.N_2C_3}$ is the most stable macrocycle followed by $\mathbf{Zn.1.N_2C_4}$ (1.4 kcal·mol$^{-1}$ higher in energy) and $\mathbf{Zn.1.N_2C_2}$ (0.8 kcal·mol$^{-1}$ higher in energy than the latter), with $\mathbf{Zn.1.N_2C_5}$ being the least stable. Comparison of structural parameters obtained from the solid state structures may provide an indication as to the origin of the stability sequence of these metallo-macrocycles (Figure 6).

These data indicate that the diamine which seems to fit best, when compared to the structural parameters of **Zn.1** (Figure 2), is $\mathbf{N_2C_2}$. The distance $C_2-C_5$ and the pinching angle $\alpha$ are very close to those of **Zn.1**, so that $\mathbf{Zn.1.N_2C_2}$ might appear the most stable macrocycle. However, closer analysis indicates that the diimine presents a deformation of $C_1C_2N_4$ and $C_2N_4C_3$ angles, as well as of the $C_4N_5C_5$ and $N_5C_5C_6$ angles which should all be ~120°. The parameter used to quantify this effect is $\alpha'-\alpha''$. A direct correlation can thus be observed between this parameter and the stability of the metallo-macrocycles deduced from competition experiments in solution. The weaker the bending effect, the more stable the respective metallo-macrocycle. Thus, accommodation of the diamine within the structure of the final metallo-macrocycle drives the selection process. Increasing the diamine length leads to an increase in the size of the macrocycle. Along the series, $Zn-N_4$ displays the largest distance increase suggesting that this bond is the weakest coordination bond, in agreement with the dissymmetry introduced by the central hydrazone unit.[94]

**2.2.2. Metal Ion-Dependent Geometrical Selection of Diamines. Cases of Hg.1 and Pb.1.** Under the same conditions as those above, we investigated the self-assembly through imine condensation of the same diamines with the U-shaped metal complex **Hg.1**. Addition of $\mathbf{N_2C_2}$ onto **Hg.1** did not result in the formation of the corresponding metallo-macrocycle, even after extensive heating. Since **Hg.1** has a wider U shape, it is probably too difficult to accommodate such a small diamine in the corresponding metallo-macrocycle. However, $\mathbf{Hg.1.N_2C_3}$, $\mathbf{Hg.1.N_2C_4}$, and $\mathbf{Hg.1.N_2C_5}$ were readily formed as the main products after mixing the corresponding diamine with **Hg.1**, as shown by $^1$H NMR spectroscopy, MALDI-TOF mass spec-

(93) The presence of the central hydrazone unit makes the whole molecule dissymmetric. Therefore the two imines do not have the same reactivity towards a nucleophile. The one on the pyridine aldehyde side must be much more prone to attack from nucleophiles than the one on the pyridine hydrazine side. Another set of crystals was also obtained and investigated by X-ray diffraction. The data were of low quality but indicated that the structure was indeed that of the macrocyclic diimine $\mathbf{Zn.1.N_2C_2}$.

(94) The presence of the central hydrazone unit makes the whole molecule dissymmetric. Therefore the two hemi-aminals do not have the same reactivity. The one on the pyridine aldehyde side is expected to be more stable than that on the pyridine hydrazine side.

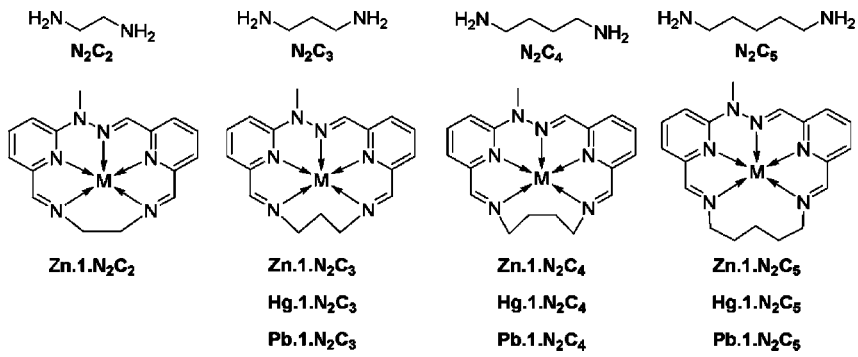


***Figure 3.*** Diamines used and their respective metallo-macrocycles formed through double imine condensation with **M.1**.

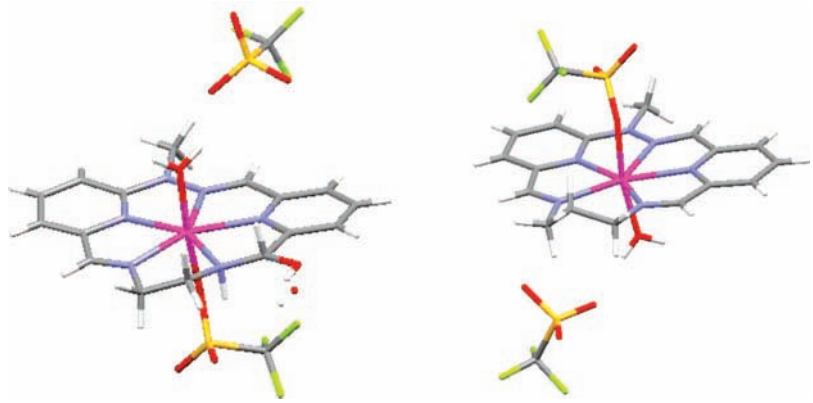

***Figure 4.*** Solid state structures of the monohemiaminal of the **Zn.1.$N_2C_2$** metallo-macrocycle (left) and of the **Zn.1.$N_2C_3$** metallo-macrocycle (right), obtained from X-ray crystallography.

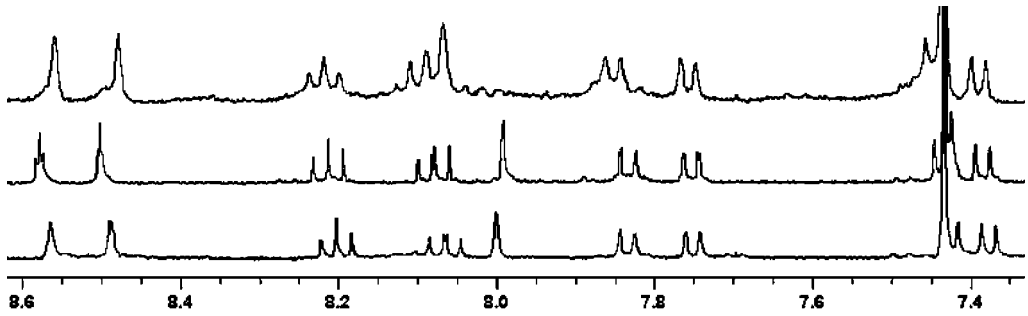


***Figure 5.*** $^1$H NMR spectra showing the selection operated by **Zn.1** between **$N_2C_4$** and **$N_2C_5$**, in $CDCl_3/CD_3CN$ 6/4 at 5 mM concentration. (Bottom) competition experiment between **$N_2C_4$** and **$N_2C5$**, spectrum recorded after a few hours at room temperature; (middle) macrocycle **Zn.1.$N_2C_4$**; (top) macrocycle **Zn.1.$N_2C_5$**. The two singlets at 8.5−8.6 ppm correspond to the imine protons, and the singlet at 8.0−8.1 ppm to the C*H* proton of the hydrazone.

trometry, and X-ray diffraction analysis of **Hg.1.$N_2C_4$** (Supporting Information). As an example, a competition experiment was performed between **$N_2C_3$** and **$N_2C_5$** which showed the selection of **$N_2C_3$** forming **Hg.1.$N_2C_3$** (Supporting Information).

With **Pb.1**, which has an even wider U shape, addition of **$N_2C_2$** resulted in the formation of a precipitate which MALDI-TOF mass spectrometry analysis revealed to be the [2 + 2] metallo-macrocycle, the small size of the diamine forcing the system to generate a constitution other than the [1 + 1] species. Addition of **$N_2C_3$** onto **Pb.1** led after extensive heating to the complete formation of a single diimine compound identified as the [1 + 1] metallo-macrocycle by MALDI-TOF mass spectrometry, which was confirmed in the solid state by X-ray diffraction analysis (Figure 7).

The structure shows that, due to the rather small size of the 16-membered macrocyclic ligand, the larger lead(II) cation is displaced out of the macrocyclic plane. Similarly, addition of **$N_2C_4$** or **$N_2C_5$** onto **Pb.1** resulted in the formation of their corresponding [1 + 1] metallo-macrocycles, respectively, **Pb.1.$N_2C_4$** and **Pb.1.$N_2C_5$**. As an example, a competition experiment was performed between **$N_2C_4$** and **$N_2C_5$** which showed complete selection of the longer **$N_2C_5$** forming **Pb.1.$N_2C_5$** (Supporting Information). Thus the presence of the large lead metal ion favors larger macrocyclic species over smaller ones.

The results above demonstrate that the nature of the metal ion can regulate the selection features of the U-shaped metal complexes toward complementary diamines through modification of geometrical features in line with the relative size of the metal cation.

**2.2.3. Coordination-Induced Selection of Diamines.** Selection of a binding site containing diamines may be induced by direct coordination to the metal cation. To this end, competition experiments were performed with diamines having the same

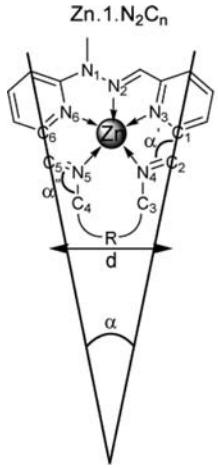


| Diamine | Distances (Å) | | | | | | Angles (°) | |
|---|---|---|---|---|---|---|---|---|
| | Zn-$N_2$ | Zn-$N_3$ | Zn-$N_4$ | Zn-$N_5$ | Zn-$N_6$ | d ($C_2$-$C_5$) | α | α'–α" |
| $N_2C_2$ | 2.33 | 2.17 | 2.26 | 2.16 | 2.17 | 5.19 | 27.7 | -6.5 |
| $N_2C_3$ | 2.44 | 2.24 | 2.32 | 2.22 | 2.24 | 5.44 | 24.1 | 4.3 |
| $N_2C_4$ | 2.40 | 2.20 | 2.47 | 2.20 | 2.24 | 5.47 | 22.5 | 5.2 |
| $N_2C_5$ | 2.35 | 2.24 | 2.73 | 2.24 | 2.19 | 5.63 | 21.5 | 8.6 |

***Figure 6.*** Comparison of structural characteristics between the metallo-macrocycles obtained from **Zn.1** and various diamines. The data reported for $N_2C_2$ were measured on the crystal structure of the monohemiaminal (see Figure 4). The α′−α″ values are the mean of the two values measured at both imine bonds in the crystal structures.

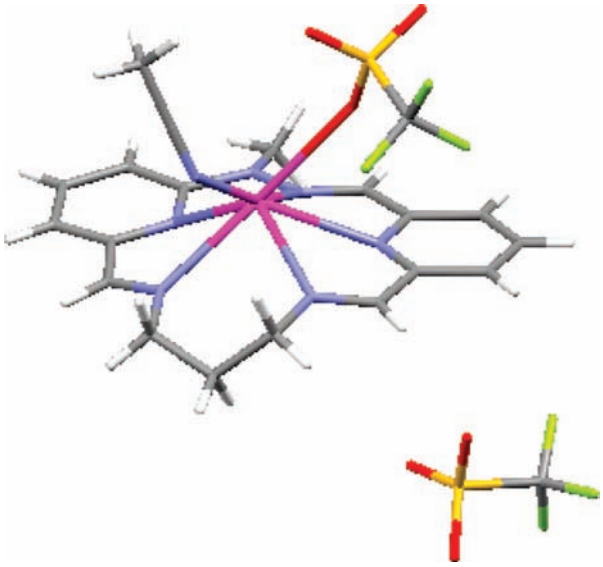

***Figure 7.*** Solid state structure of **Pb.1.$N_2C_3$**.

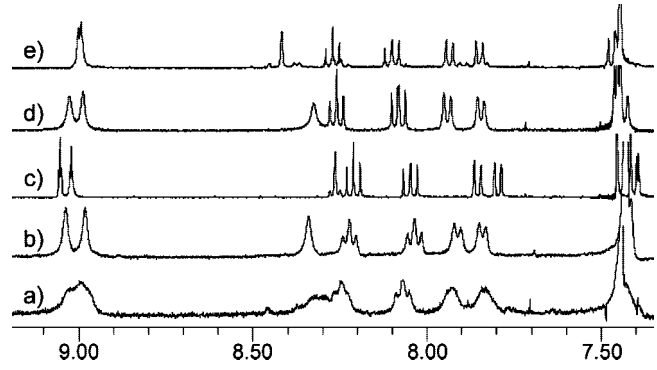


***Figure 8.*** $^1$H NMR spectra showing the selection operated by **Pb.1** between $N_2O$ and $N_2C_5$, in $CDCl_3/CD_3CN$ 6/4 at 5 mM concentration. (a) After addition of 1 equiv of $Pb(OTf)_2$ to an equimolar mixture of **1**, $N_2O$, and $N_2C_5$; (b) (a) cooled to −50 °C; (c) **Pb.1.$N_2O$**; (d) addition of 1 equiv $N_2C_5$ to **Pb.1.$N_2O$**; (e) **Pb.1.$N_2C_5$**. The broadening of the signals in (a) may be related to the occurrence of exchange processes (see text and (b)). The two signals at about 9.0 ppm correspond to the imine protons.

length but with one of them containing an atom capable of interacting with the metal ion (Scheme 3). $N_2C_5$ and $N_2O$ separately form the corresponding [1 + 1] metallo-macrocycles with **Zn.1** and **Pb.1**. Using a 1:1 mixture of these diamines did not give a clear indication suggesting a possible selection in the case of zinc. However, in the case of lead, $^1$H NMR spectroscopy provided evidence of a selection occurring in favor of $N_2O$. The difference between these two ions may reflect a difference in both structural (see above) and coordination features. Lead(II) is large and can accommodate more diverse coordination geometries than zinc(II). The $^1$H NMR spectrum of the competition experiment between $N_2C_5$, $N_2O$, and **Pb.1** required cooling to −50 °C to observe sharp signals demonstrating that selection of $N_2O$ had occurred (Figure 8).

The broadening of the NMR signals at room temperature may be explained by coordination exchanges operated on **Pb.1.$N_2O$** by binding of the surrounding nonselected free diamine $N_2C_5$ to free sites on the metal ion. This is supported by the fact that addition of $N_2C_5$ onto **Pb.1.$N_2O$** induces an immediate change in the chemical shifts (Figure 8), whereas, on addition of $N_2O$ to **Pb.1.$N_2C_5$**, the formation of **Pb.1.$N_2O$** through transimination[56] is much slower, requiring hours to reach the thermodynamic state (Supporting Information). Furthermore, cooling of **Pb.1.$N_2O$** did not change its NMR spectrum, indicating that the broadening observed in the competition experiment has an intermolecular origin and is not due to intramolecular (conformational) dynamic processes.

Competition experiments were also performed between $N_2C_5$ and $N_2NH$ (2,2′-diaminodiethylamine). The use of lead metal salt drives the system to the selection of the coordinative diamine $N_2NH$ as shown by $^1$H NMR spectroscopy (Supporting Information). X-ray diffraction analysis confirmed that the observed selection was indeed due to an additional coordination of the central metal ion. The solid state structure of **Pb.1.$N_2NH$** displayed in Figure 9 shows indeed six coplanar coordination bonds. Moreover, crystallization of a mixture of **Pb.1.$N_2O$** and DMAP provided single crystals for which the solid state structure, obtained by X-ray crystallography, revealed the axial coordination of an external agent.[95]

The case of zinc is peculiar. Whereas the macrocycle **Zn.1.$N_2C_5$** is self-assembled from its components by imine

(95) Such interaction, which was previously discussed, was also shown to occur in solution. $^1$H NMR titration gave changes of chemical shifts of the metallo-macrocycle **Pb.1.$N_2O$** upon addition of DMAP, imidazole, or pyridine (see Supporting Information).

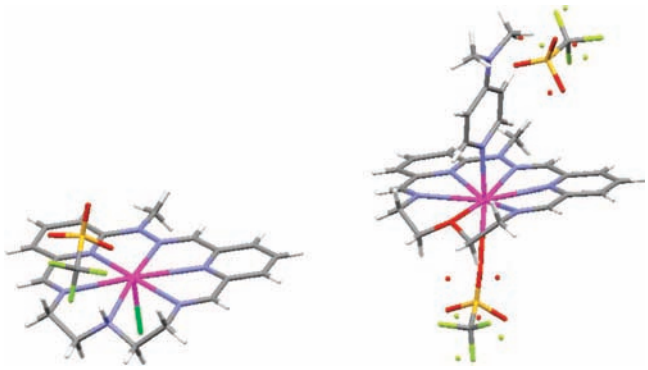

***Figure 9.*** Solid state structures of **Pb.1.$N_2$NH** showing the coordination bond between NH and the central lead ion (left) and solid state structure of the adduct between **Pb.1.$N_2$O** and DMAP showing the axial interaction with an additional coordinating molecule (right).

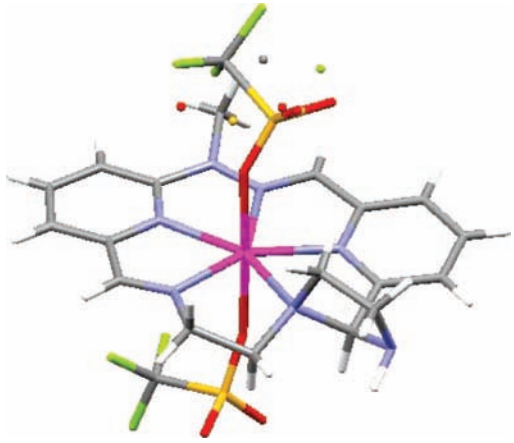

***Figure 10.*** Solid state structures of **Zn.1.$N_2$NH** showing its contracted aminal structure.

formation as previously described,[81] the addition of **$N_2$NH** to **Zn.1** did not result in the diimine metallo-macrocycle formation but rather in a size adaptation by intramolecular reaction with contraction to a smaller metallo-macrocycle containing an aminal moiety (Figure 10), a process already reported in the literature.[56]

Interestingly, the aminal moiety is formed at the more reactive imine bond, the one on the pyridine aldehyde side (see above). A competition experiment carried out between **$N_2C_5$** and **$N_2$NH** shows that **Zn.1** is capable of selecting **$N_2$NH** by forming the compact metallo-macrocycle **Zn.1.$N_2$NH** (Supporting Information).

In summary, in addition to the previously described geometrical selection, the nature of the diamine, and in particular the presence of a coordinating site, also induces component selection.

**2.3. Diamine-Dependent Selection of Metal Ions.** We have shown above that the nature of the metal ion confers particular geometrical features to the metal complexes **M.1** and therefore induces selection of a particular diamine from a mixture of competing diamines. Would the reverse be possible? Would the presence of only one diamine impose the selection of a particular metal ion from a mixture of different metal ions through the formation of a preferred metallo-macrocyclic architecture (Scheme 4)?[96]

(96) Piotrowski, H.; Polborn, K.; Hilt, G.; Severin, K. *J. Am. Chem. Soc.* **2001**, *123*, 2699–2700.

***Scheme 4.*** Representation of the Selection Process Operated by the Self-Assembled Macrocycle between Two Different Metal Ions

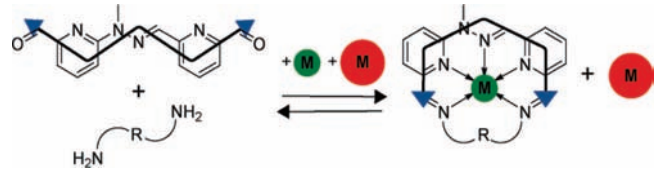


We investigated first the inherent preference of the ligand **1** for a particular metal ion. Addition of **1** to an equimolar mixture (1.0 equiv of each) of zinc triflate and lead triflate gave 55% **Zn.1** and 45% of **Pb.1**. Competition experiments between zinc triflate and mercury triflate led to the thermodynamic formation of 79% of **Hg.1** and 21% of **Zn.1** after one day of heating at 60 °C, since **Hg.1** was found to be kinetically more inert than **Zn.1** and **Pb.1**. Similarly, lead triflate and mercury triflate yielded ca. 90% of **Hg.1** and 10% of **Pb.1** after one day of heating at 60 °C. In summary, ligand **1** has a slight preference for a mercury(II) metal cation. The metal complex **Zn.1** is then 1.6 kcal·mol$^{-1}$ less stable, and **Pb.1** is the least stable, by 0.2 and ca. 2.0 kcal·mol$^{-1}$ compared to **Zn.1** and **Hg.1**, respectively. Addition of **$N_2C_5$** to the mixture of **1**, zinc triflate and lead triflate gave, respectively, 30% and 70% of metallo-macrocycles **Zn.1.$N_2C_5$** and **Pb.1.$N_2C_5$** demonstrating that the condensation of the diamine reversed the relative proportions by inducing the incorporation of lead(II) at the expense of zinc(II) cations (Scheme 5 and Supporting Information). This transmetalation process, which occurs at room temperature, was also demonstrated by the addition of lead triflate to **Zn.1.$N_2C_5$** that resulted in the same constitutional equilibrium. On the other hand, addition of **$N_2$O** to the equimolar mixture of **1**, zinc triflate, and lead triflate yielded quantitatively the lead macrocycle **Pb.1.$N_2$O** due to the stabilization provided by the additional coordinating site (see above), thus leaving zinc ions in solution (Scheme 5 and Supporting Information). Conversely, the use of a shorter diamine like **$N_2C_2$** and **$N_2C_4$** led to the quantitative formation of the zinc macrocycles **Zn.1.$N_2C_2$** and **Zn.1.$N_2C_4$**, respectively, due to a size selection imposed by the smaller cavity of the [1 + 1] macrocyclic species (Scheme 5 and Supporting Information).

Similar competition experiments were carried out between zinc triflate and mercury triflate. Addition of 1 equiv of either **$N_2C_2$** or **$N_2C_3$** to an equimolar mixture of **1**, zinc triflate, and mercury triflate gave ($^1$H NMR) the corresponding zinc macrocycle as the main product in the first case and in 80% versus 20% of the corresponding mercury macrocycle in the second case (Supporting Information). On the other hand, addition of 1 equiv of either **$N_2C_4$** or **$N_2C_5$** to an equimolar mixture of **1**, zinc triflate, and mercury triflate yielded ($^1$H NMR) the corresponding mercury macrocycles as the main products in both cases (Supporting Information). The same kind of competition experiments were performed between mercury triflate and lead triflate. Addition of **$N_2C_4$**, **$N_2C_5$**, or **$N_2$O** to an equimolar mixture of **1**, mercury triflate, and lead triflate resulted in the preferential formation of the mercury macrocycles (Supporting Information). To confirm that such a selection is of a thermodynamic nature, 1 equiv of mercury triflate was added to a solution of **Pb.1.$N_2$O** and complete transmetalation to **Hg.1.$N_2$O** was observed after one day at room temperature.

In summary, the condensation of a specific diamine can induce the selection of a particular metal ion that leads to the most stable [1 + 1] metallo-macrocycle. The relative stabilities

***Scheme 5.*** Representation of the Influence of a Particular Diamine on the Metal Ions Preferences of the Final Macrocycles[a]

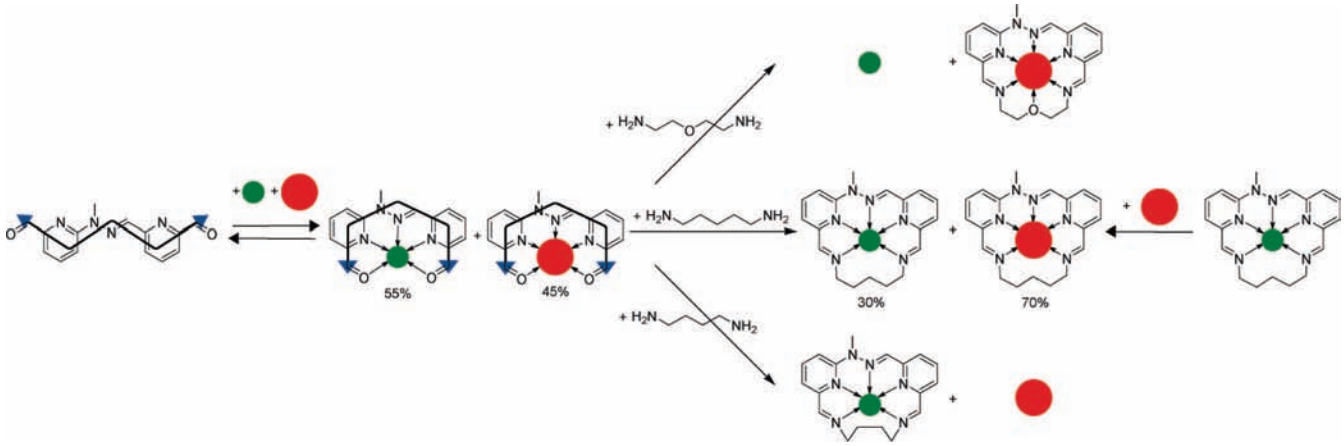


[a] The smaller circle represents zinc(II) ion and the larger one lead(II) ion.

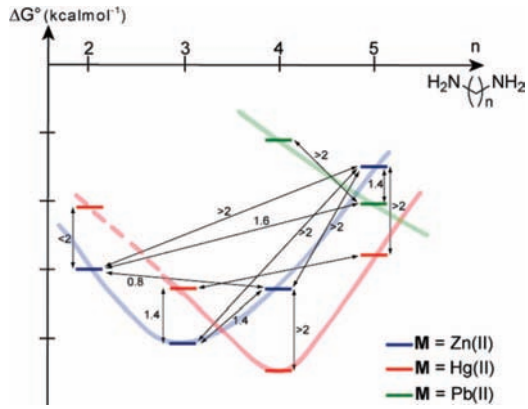


***Figure 11.*** Representation of the standart free energy of the metallo-macrocycles as a function of the length of the diamine with three different metal ions, zinc, mercury, and lead. The $\Delta(\Delta G°)$ values indicated were obtained from competition experiments and measured by $^1$H NMR spectroscopy (see text).

may be operationally related to the fit between the metal ion and the macrocyclic structure, which itself depends on the nature of the diamine. Figure 11 gives a representation of the metallo-macrocycles studied as a function of the incorporated diamine, based on the competition experiments described above.

**2.4. Constitutional Coevolution in Response to Reciprocal Metal Ion/Diamine Effects.** The data above demonstrate that a reciprocal relationship exists between the metal ion and the diamine: the metal ion influences the selection of a complementary diamine from a pool of diamines, and conversely a given diamine may favor the selection of a particular metal ion from a mixture of different metal salts. As a consequence, it became of interest to investigate the correlated evolution of the constitution of systems containing *both* different metal cations and different diamines (Scheme 6).

For example, an equimolar mixture of **1**, zinc triflate, lead triflate, $\mathbf{N_2C_5}$, and $\mathbf{N_2C_2}$ evolves until reaching a constitutional state made up of 78% $\mathbf{Zn.1.N_2C_2}$ and 22% $\mathbf{Pb.1.N_2C_5}$ (Figure 12). In principle, four differents macrocycles could have been formed, but only two emerged from this virtual dynamic library.[32] These two amplified covalent assemblies correspond to the combination of components that generates the thermodynamically most stable state of the system. Thus, the short diamine $\mathbf{N_2C_2}$ is associated with the small metal ion zinc, whereas the larger diamine $\mathbf{N_2C_5}$ is associated with the larger metal ion lead. In the system studied, the two constituents expressed, $\mathbf{Zn.1.N_2C_2}$ and $\mathbf{Pb.1.N_2C_5}$, are in an agonistic relationship[97] with one another and in an antagonistic relationship[97] with the two other possible combinations $\mathbf{Zn.1.N_2C_5}$ and $\mathbf{Pb.1.N_2C_2}$. This agonistic feature also ensures that the amplification is quantitative.

A striking case is provided by the observation that an equimolar mixture of **1**, zinc triflate, lead triflate, $\mathbf{N_2C_5}$, and $\mathbf{N_2O}$ spontaneously evolves toward the formation of only $\mathbf{Pb.1.N_2O}$. From the four possible products, the only one formed results from the selection of the components lead ion and $\mathbf{N_2O}$ (Figure 13), which provide additional coordination interactions (see above). Such a selection also occurs on addition of 1 equiv of $\mathbf{N_2O}$ to the equilibrated mixture of $\mathbf{Zn.1.N_2C_5}$ and $\mathbf{Pb.1.N_2C_5}$ (see above) which leads, by transimination and then by an induced transmetalation, to the exclusive formation of $\mathbf{Pb.1.N_2O}$.

Another example demonstrates the coevolution behavior of such dynamic systems. As previously shown, addition of $\mathbf{N_2C_5}$ to an equimolar mixture of **1**, zinc triflate, and mercury triflate leads to the selective formation of $\mathbf{Hg.1.N_2C_5}$. Addition of 1 equiv of $\mathbf{N_2C_2}$ leads to recomposition of the system toward the major formation (90%) of $\mathbf{Zn.1.N_2C_2}$ along with the minor presence (10%) of $\mathbf{Hg.1.N_2C_5}$, thus showing that the system evolves by using two dynamic processes, metal coordination and imine formation, to generate the most stable species by incorporating the components which display a reciprocal stabilization (Supporting Information).

These examples illustrate the complex behavior presented by constitutionally dynamic systems. Since the constituents are labile, they can evolve until achieving integration of the elements which, by interacting with each other, adapt the whole structure to the internal and external conditions.

**2.5. Constitutional Adaptation in Response to Shape Changes. 2.5.1. Two Diamines and a Single Switching Unit 1.** It has been shown above that the U-shaped complex **Pb.1** discriminates between $\mathbf{N_2C_5}$ and $\mathbf{N_2O}$, due to an increased stability by coordination to the oxygen site in the corresponding [1 + 1] metallo-macrocycle $\mathbf{Pb.1.N_2O}$. An opposite selection occurs in the metal-free state. Addition of ligand **1** to an equimolar mixture of $\mathbf{N_2C_5}$ and $\mathbf{N_2O}$ in $CDCl_3/CD_3CN$ 6/4 yielded a precipitate containing products from **1** and $\mathbf{N_2C_5}$ while

(97) Giuseppone, N.; Lehn, J.-M. *Chem.—Eur. J.* **2006**, *12*, 1715–1722.

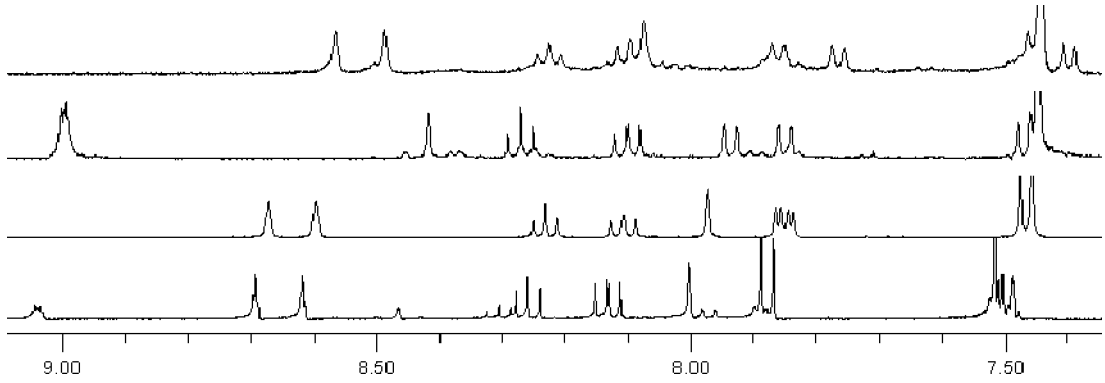


***Figure 12.*** $^1$H NMR spectra showing the coevolution from an equimolar mixture of **1**, zinc triflate, lead triflate, $\mathbf{N_2C_2}$, and $\mathbf{N_2C_5}$, in $CDCl_3/CD_3CN$ 6/4 at 5 mM concentration. From bottom to top: competition experiment (78% $\mathbf{Zn.1.N_2C_2}$, 22% $\mathbf{Pb.1.N_2C_5}$), spectrum recorded after 6 days at 65 °C; $\mathbf{Zn.1.N_2C_2}$; $\mathbf{Pb.1.N_2C_5}$; $\mathbf{Zn.1.N_2C_5}$. The signals between 8.5 and 9.1 ppm correspond to the imine protons. Two distinct singlets are observed for the zinc metallo-macrocycles, whereas in the case of the lead metallo-macrocycle they overlap and a broad signal is observed.

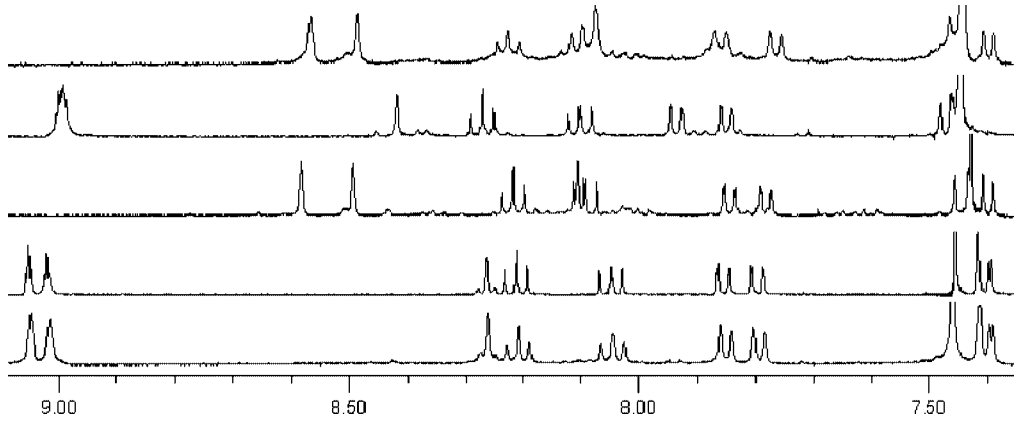


***Figure 13.*** $^1$H NMR spectra showing the coevolution of an equimolar mixture of **1**, zinc triflate, lead triflate, $\mathbf{N_2C_5}$, and $\mathbf{N_2O}$, in $CDCl_3/CD_3CN$ 6/4 at 5 mM concentration toward the generation of $\mathbf{Pb.1.N_2O}$. From bottom to top: competition experiment, spectrum recorded after 3 days at 60 °C; $\mathbf{Pb.1.N_2O}$; $\mathbf{Zn.1.N_2O}$; $\mathbf{Pb.1.N_2C_5}$; $\mathbf{Zn.1.N_2C_5}$. The signals between 8.5 and 9.1 ppm correspond to the imine protons.

***Scheme 6.*** Representation of a Co-Evolution Process Where Two Given (Diamine, Metal Ion) Couples Are Selected from a Pool of Diamines and Metal Salts, As a Result of the Interactions Imposed by the Shape of the Complexed Dialdehyde

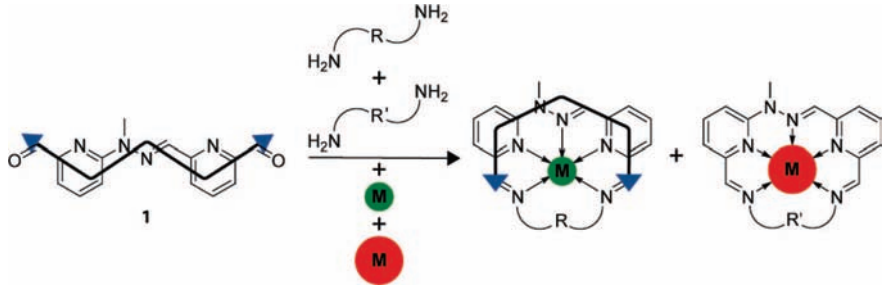


the remaining diamine $\mathbf{N_2O}$ stayed in solution, a behavior indicative of selection under phase change (Supporting Information).

As reported, **1** reacts with $\mathbf{N_2C_5}$ or $\mathbf{N_2O}$ to give, mainly for the first diamine and exclusively for the second one, at a 5 mM concentration in $CDCl_3/CD_3CN$ 6/4 the corresponding [2 + 2] macrocycles.[81] Whereas the latter was nicely soluble in this medium, the former precipitated out from solution. It is this phase change that drives the observed selection process in favor of $\mathbf{N_2C_5}$ at the expense of $\mathbf{N_2O}$ which stays free in solution. Indeed, in $CDCl_3$, where all species are soluble, MALDI-TOF mass spectrometry analysis revealed the presence, as expected, of the [2 + 2] macrocycles formed from **1** plus $\mathbf{N_2C_5}$ and **1** plus $\mathbf{N_2O}$ but also the hetero [2 + 2] macrocycle containing both diamines, while $^1$H NMR spectroscopy clearly showed that both diamines remained partially free in solution (since 1 equiv of each diamine was added), thus pointing to the nonselective self-assembly in solution (Supporting Information).

The two different shape states of **1**, metal-free and complex, thus displayed opposite selectivities as a consequence of two orthogonal effects, phase change and coordination. It is also possible to switch reversibly between these selective constitutional states by addition/removal of the metal ion. Thus, addition of lead triflate to the heterogeneous system containing $\mathbf{1_2.(N_2C_5)_2}$ as a precipitate and free $\mathbf{N_2O}$ in solution results in the complete solubilization of the material and in the inversion of the selection, thus forming the [1 + 1] metallo-macrocycle $\mathbf{Pb.1.N_2O}$ and leaving free $\mathbf{N_2C_5}$ in solution (Scheme 1A).

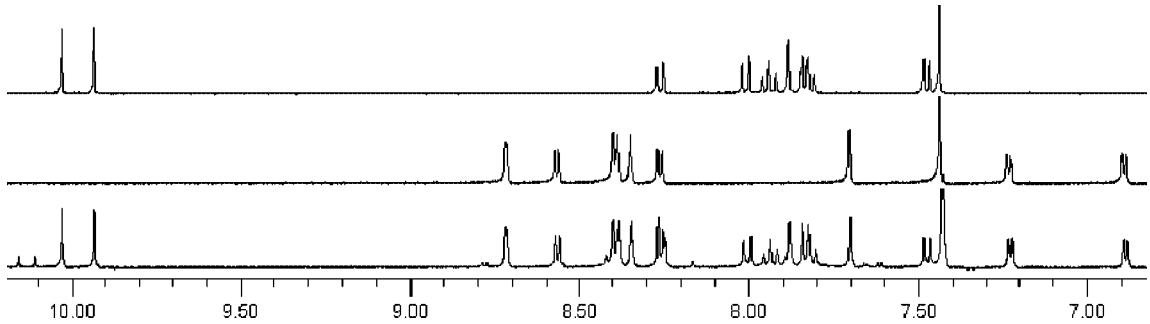


***Figure 14.*** $^1$H NMR spectra showing the selective self-assembly process resulting from an equimolar mixture of **1**, **2**, and $\mathbf{N_2C_5}$ in $CDCl_3/CD_3CN$ 6/4 at 5 mM concentration. From bottom to top: mixture after 2 days at room temperature; macrocycle $\mathbf{2.N_2C_5}$; **1**. The signals at ~10 ppm correspond to the aldehyde protons.

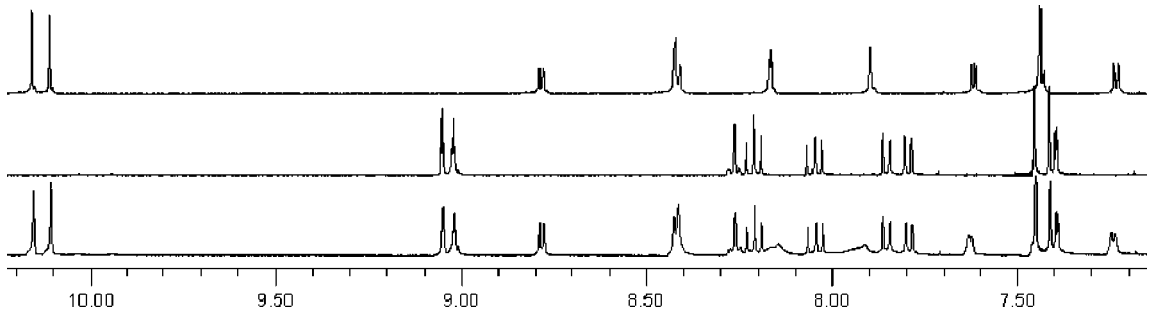


***Figure 15.*** $^1$H NMR spectra showing the selective condensation resulting from an equimolar mixture of **1**, **2**, and $\mathbf{N_2O}$ and lead triflate in $CDCl_3/CD_3CN$ 6/4 at 5 mM concentration. From bottom to top: mixture after 1 day at room temperature; macrocycle $\mathbf{Pb.1.N_2O}$; **2**. The signals at ~10 ppm correspond to the aldehyde protons, and those at ~9 ppm correspond to the imine protons.

**2.5.2. Two Switching Units 1, 2, and a Single Diamine.** Another example of such an adaptive behavior in response to morphological switching processes is provided by a mixture of dialdehydes **1** and **2**, which represents a morphologically complex system since **1** has a W shape whereas **2** has a U shape. Addition of a diamine should lead to a preferential self-assembly with the best partner (Scheme 1B). $^1$H NMR spectroscopy showed that addition of either $\mathbf{N_2C_5}$ or $\mathbf{N_2O}$ to an equimolar mixture of **1** and **2** yields, respectively, the macrocycles $\mathbf{2.N_2C_5}$ and $\mathbf{2_2.(N_2O)_2}$ showing that these diamines both select the U-shaped dialdehyde **2** at the expense of the W-shaped **1** (Figure 14 and Supporting Information).

We then investigated the constitutional reaction of this system upon addition of a metal ion. Addition of 1 equiv of lead triflate to a mixture of **1** and either $\mathbf{2.N_2C_5}$ or $\mathbf{2_2.(N_2O)_2}$ resulted, after a few tens of minutes, in the quantitative formation of free **2** and, respectively, either $\mathbf{Pb.1.N_2C_5}$ or $\mathbf{Pb.1.N_2O}$ (Figure 15 and Supporting Information).

Thus, the covalent dynamic system is able to adapt its constituents to the morphology of the dialdehyde, from an initial state governed solely by shape to a second one where the shape change of **1**, from W to U, allows additionally for coordination to the imines, a major contributing factor (see hereafter).

The complexation of a mixture of ligands **1** and **2** was then studied by $^1$H NMR spectroscopy (Supporting Information). Due to the fast exchange regime compared to the NMR time scale, quantification is not possible but qualitative analysis shows the formation of **Pb.1** and $\mathbf{Pb.2_2}$ in fast exchange with free ligands **1** and **2**. Addition of 1 equiv of either $\mathbf{N_2O}$ or $\mathbf{N_2C_5}$ results in the quantitative formation of free **2** and of $\mathbf{Pb.1.N_2O}$ and $\mathbf{Pb.1.N_2C_5}$, respectively. This is mainly due to the presence of the metal ion in **Pb.1** which ensures stabilization of these imines by coordination to the N sites. Indeed, an equimolar mixture of **1** and **2** gives, after addition of 2.0 equiv of *n*-octylamine, $\mathbf{NC_8}$, a statistical mixture of several mono- and diimines, whereas further addition of 1 equiv of lead triflate leads to the major formation of $\mathbf{Pb.1.(NC_8)_2}$ and free **2** (Supporting Information). Thus coordination shifts all complexation and imine formation equilibria. The U-shaped complex **Pb.1** is not quantitatively present in the mixture of ligands **1**, **2**, and lead triflate, whereas the addition of either $\mathbf{N_2O}$ or $\mathbf{N_2C_5}$ leads to a quantitative formation of the corresponding metallo-macrocycles (Scheme 1B). The addition of zinc triflate to the mixture of **1** and **2** was also studied but led to a more complicated behavior (Supporting Information).

Furthermore, addition of cryptand [2.2.2] to sequestrate the lead cation induces the whole system to go back to its original constitution characteristic of the metal-free states (data not shown).

**2.5.3. Monoamine, Diamine, and Two Switching Units 1, 2.** A more complex example shows the importance of macrocyclic type metal ion coordination on the self-assembly processes (Scheme 7).

Addition of 2 equiv of *n*-octylamine, $\mathbf{NC_8}$, and 1 equiv of $\mathbf{N_2O}$ to an equimolar mixture of **1** and **2** yields a selective thermodynamic state where the monoamine has reacted with the W-shaped dialdehyde and the diamine with the U-shaped one. Addition of 1 equiv of lead triflate and 2 equiv of imidazole[98] to this mixture results in the quantitative formation of $\mathbf{Pb.1.N_2O}$ and $\mathbf{2.(NC_8)_2}$ by an imine swapping induced by

(98) After addition of lead triflate, imine hydrolysis was observed. This can be explained by the fact that additional imines can coordinate the metallo-macrocycle in its axial position (see text) and therefore activate the imine towards a nucleophilic attack from residual water. Imidazole can prohibit that by occupying the axial position of the metallo-macrocycle as it has been previously proven (see text). It also makes the medium more basic which helps the formation of imines.

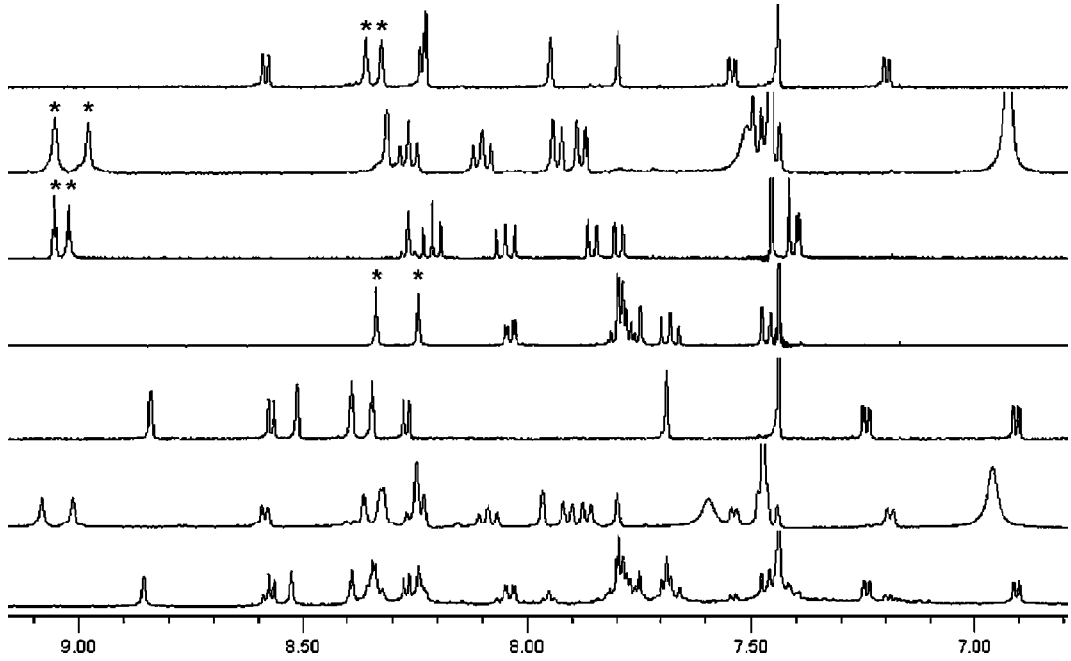


***Figure 16.*** Constitutional adaptation, by imine swapping, induced by morphological changes. $^1$H NMR spectra in $CDCl_3/CD_3CN$ 6/4 at 5 mM concentration. From bottom to top: equimolar mixture of **1**, **2**, $\mathbf{N_2O}$, and 2.0 equiv of $\mathbf{NC_8}$, after 2 days at room temperature; after addition of 1 equiv of lead triflate and 2 equiv of imidazole to the previous system; $\mathbf{2_2.(N_2O)_2}$; $\mathbf{1.(NC_8)_2}$; $\mathbf{Pb.1.N_2O}$; $\mathbf{Pb.1.N_2O}$ with 2 added equiv of imidazole; $\mathbf{2.(NC_8)_2}$. The signals corresponding to the imine protons are marked with a star.

***Scheme 7.*** Illustration of an Adaptation Process Induced by Metal Ion Coordination and Molecular Shape Changes and Operating through Imine Swapping

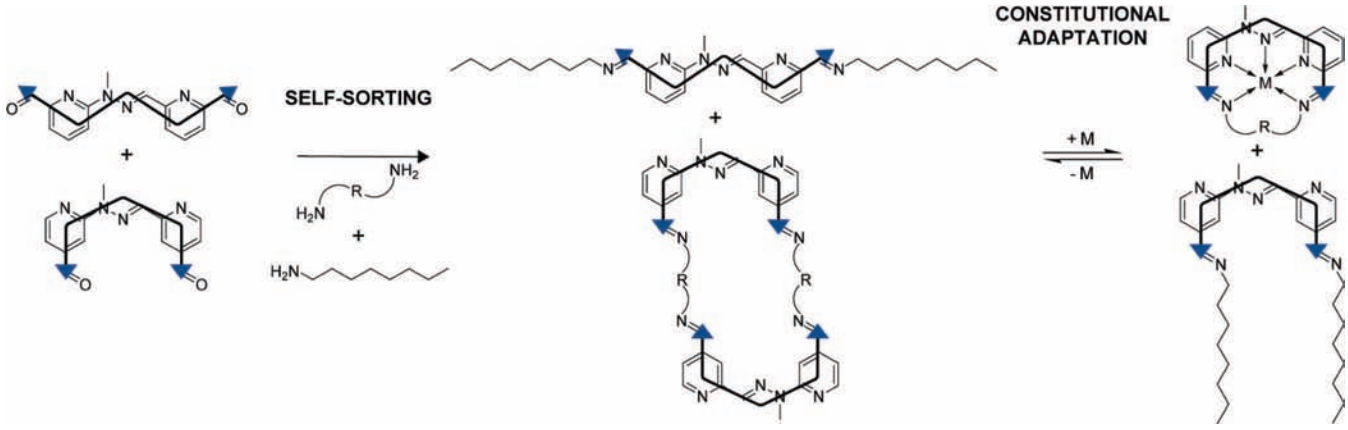


both metal ion coordination and morphological changes (Figure 16). When $\mathbf{N_2O}$ is replaced by $\mathbf{N_2C_5}$, the mixture of reactants yields $\mathbf{1.(NC_8)_2}$ and $\mathbf{2.N_2C_5}$, and subsequent addition of 1 equiv of lead triflate simply results in a complexation to give $\mathbf{Pb.1.(NC_8)_2}$ and $\mathbf{2.N_2C_5}$ without a constitutional change (data not shown). This control experiment points to the importance of the additional coordination site, provided by the oxygen atom in $\mathbf{Pb.1.N_2O}$, in the observed constitutional adaptation.

These results show the importance of additional coordination in the selection of the component leading to a constitutional adaptation induced by metal ion binding.

## 3. Conclusions

The present results demonstrate that molecular morphology can be translated into a specific constitution by selection of the components which fit best within the final architecture. Thus, diamines having different lengths self-assemble with a dialdehyde with a well-defined shape to form cyclic structures of different energies. Combining solution state and solid state results has allowed deciphering the origin of this thermodynamic selection. The energetic bias, due to structural and coordination differences, lead to the selection of the most appropriate diamine from a mixture. Since the exact geometrical features of the dialdehyde−metal complex are a direct consequence of the nature of the metal ion, the energetic profiles of the macrocyclic species formed depend upon the metal ion used. In addition, a "reverse" selection was found to occur; i.e., a diamine can play the role of the effector and then induce the selection of one particular metal ion from a mixture, one which fits best into the final macrocyclic structure. Starting from a mixture of diamines having the same length, other factors, such as coordination and phase separation, play an important role in the selection of components. A similar reciprocal influence between diamines and metal ions has been found. As a result of these mutual interactions, the dynamic system undergoes coevolution toward the entities that incorporate the components

leading to the most stable structure. Since dialdehyde **1** is a morphological switch, interconverting W- and U-shaped states, component selection could be switched on and off simply by addition or removal of the metal ion which both induces shape change and introduces coordination interactions. Moreover, under the action of phase separation and coordination as two orthogonal parameters, the system displayed constitutional adaptation behavior; i.e., component selection was switched between two different states by metal ion binding and shape switching of the dialdehyde. A mixture of the two different morphological switches **1** and **2** selectively reacted with a mixture of mono- and diamine to yield a self-sorted state, and subsequent addition of a metal ion led to a complete conversion to a state of different constitution. Finally, one may remark that, in view of the large geometrical change involved in the W/U interconversion, the present results also represent a coupling of constitutional dynamics to mechanical motions.

In conclusion, this study demonstrates that morphological information can be used to steer the evolution of a constitutional dynamic system toward the incorporation and/or decorporation of particular components, in response to shape change of molecular switches between two states, characterized both by their geometry and by their coordination features. The implementation of morphological switches in constitutional dynamic chemistry can therefore give rise to complex systems[99] presenting behaviors such as constitutional adaptation and coevolution.

## 4. Experimental Section

**4.1. General.** All reagents were purchased from commercial suppliers and used without further purifications unless otherwise noted. The syntheses of **1**, **2**, their zinc and lead complexes, macrocycles **Zn.1.N$_2$C$_4$**, **Zn.1.N$_2$C$_5$**, **Zn.1.N$_2$O**, **2.N$_2$C$_5$**, **2$_2$.(N$_2$O)$_2$**, and diimines **1.(NC$_8$)$_2$** and **2.(NC$_8$)$_2$** were previously described.[81] Metal salts were dried by gentle heating at 60 °C under vacuum for a few hours. $CDCl_3$* denotes the use of $CDCl_3$ which was filtered through basic alumina to remove traces of acidity. $^1$H NMR spectra were recorded on a Bruker Avance 400 spectrometer at 400 MHz. Chemical shifts are given in ppm. Residual solvent peaks were taken as reference ($CDCl_3$: 7.26 ppm, $CD_3CN$: 1.94 ppm).[100] The coupling constants *J* are given in Hz. Peaks are described as singlet (s), doublet (d), triplet (t), doublet of doublet (dd), multiplet (m), and broad (br). The assigned proton is italicized. When mixtures of solvent were used, the calibration was done using the residual solvent peak of $CD_3CN$ in the case of $CDCl_3$/$CD_3CN$ mixtures. 2D NMR (COSY, ROESY) were recorded on a Bruker Avance 400 spectrometer. High-Resolution ElectroSpray Ionization Mass Spectrometry (HR-ESI-MS) analyses were performed on a Bruker Micro TOF mass spectrometer at the Service de Spectrométrie de Masse, Université Louis Pasteur. The given value represents the largest peak. The observed pattern was always conformed to the theoretical pattern and is reported in the Supporting Information. MALDI-TOF analyses were performed on a Bruker AutoFlex II mass spectrometer at the Service de Spectrométrie de Masse, Université Louis Pasteur. The given value represents the largest peak. The observed pattern was always conformed to the theoretical pattern. X-ray crystallography was performed at the Service de Radiocristallographie, Université Louis Pasteur. The crystals were placed in oil, and a single crystal was selected, mounted on a glass fiber, and placed in a low temperature nitrogen stream. The X-ray diffraction data were collected on a Nonius-Kappa-CCD diffractometer with graphite monochromatized Mo Kα radiation ($\lambda$ = 0.710 73 Å), phi scans, by using a "phi-scan" type scan mode.

**4.2. Synthesis of Hg.1.** Anhydrous $Hg(OTf)_2$ (100 $\mu$L of a 30 mM solution in $CD_3CN$, 3 $\mu$mol) was added to a 5 mM solution of **1** (0.805 mg, 3 $\mu$mol) in $CDCl_3$*/$CD_3CN$ 6/4 (0.6 mL). $^1$H NMR ($CDCl_3$*/$CD_3CN$ 51/49): 10.37 (s, 1H, $H_3$), 10.27 (s, 1H, $H_{10}$), 8.56 (t, $J$ = 7.4, 1H, $H_5$), 8.42 (d, $J$ = 7.6, 1H, $H_4$), 8.38 (t, $J$ = 7.8, 1H, $H_8$), 8.25 (m, 2H, $H_2$ + $H_6$), 8.03 (d, $J$ = 7.2, 1H, $H_9$), 7.91 (d, $J$ = 8.8, 1H, $H_7$), 3.75 (s, 3H, $H_1$); HR-ESI-MS: calculated for $[C_{15}H_{12}F_3HgN_4O_5S]^+$ 619.0187, found 618.9979. Single crystals were obtained by slow diffusion of diisopropylether into a $CHCl_3$/$CH_3CN$ solution of the metal complex.

**4.3. General Procedure for the Formation of Diimine Macrocycles.** The dialdehyde **1** (3 $\mu$mol in 0.6 mL of $CDCl_3$/$CD_3CN$ 6/4) was charged in an NMR tube. Metal salt (3 $\mu$mol from a 60 mM $CDCl_3$/$CD_3CN$ 6/4 solution in the case of zinc triflate, 30 mM $CD_3CN$ solution in the case of mercury triflate, 60 mM $CD_3CN$ solution in the case of lead triflate), followed by the diamine (3 $\mu$mol in 50 $\mu$L of $CDCl_3$/$CD_3CN$ 6/4) were added.

**4.4. Zn.1.N$_2$C$_2$.** The reaction mixture was heated at 65 °C. Thermodynamic equilibrium was reached after 1 week. $^1$H NMR ($CDCl_3$*/$CD_3CN$ 6/4): 8.67 (s, 1H), 8.60 (s, 1H), 8.23 (t, $J$ = 7.8, 1H), 8.11 (dd, $J$ = 8.4, $J$ = 7.6, 1H), 7.97 (s, 1H), 7.85 (m, 2H), 7.47 (m, 2H), 4.17 (m, 4H), 3.67 (s, 3H, NC$H_3$); MALDI-TOF (THAP): calculated for $[C_{17}H_{16}F_3N_6O_3SZn]^+$ 505.024, found 505.034.

**4.5. Zn.1.N$_2$C$_3$.** The reaction mixture was heated at 65 °C. Thermodynamic equilibrium was reached after 24 h. $^1$H NMR ($CDCl_3$*/$CD_3CN$: 6/4): 8.53 (s, 1H), 8.43 (s, 1H), 8.20 (t, $J$ = 7.6, 1H), 8.07 (t, $J$ = 7.8, 1H), 7.98 (s, 1H), 7.83 (d, $J$ = 7.6, 1H), 7.76 (d, $J$ = 7.6, 1H), 7.43 (m, 1H), 7.38 (d, $J$ = 7.2, 1H), 4.16 (m, 4H, NC$H_2$), 3.66 (s, 3H, NC$H_3$), 2.15 (m, 2H); MALDI-TOF (dithranol): calculated for $[C_{18}H_{18}F_3N_6O_3SZn]^+$ 519.0405, found 519.0000.

**4.6. Hg.1.N$_2$C$_3$.** Thermodynamic equilibrium was reached after 1 day at 60 °C. $^1$H NMR ($CDCl_3$*/$CD_3CN$ 52/48): 8.74 (t, $J$ = 1.6, 1H), 8.68 (t, $J$ = 1.8, 1H), 8.31 (t, $J$ = 7.6, 1H), 8.15 (m, 1H), 8.06 (s, 1H), 7.99 (d, $J$ = 7.6, 1H), 7.90 (d, $J$ = 8.0, 1H), 7.65 (d, $J$ = 8.8, 1H), 7.51 (d, $J$ = 7.2, 1H), 4.28 (m, 4H, NC$H_2$), 3.67 (s, 3H, NC$H_3$), 2.26 (m, 2H, NCH$_2$C$H_2$); MALDI-TOF (dithranol): calculated for $[C_{18}H_{18}F_3HgN_6O_3S]^+$ 657.0819, found 656.9189.

**4.7. Hg.1.N$_2$C$_4$.** Thermodynamic equilibrium was reached after 12−24 h at room temperature. $^1$H NMR ($CDCl_3$*/$CD_3CN$: 52/48): 8.79 (s, 1H, $H_3$), 8.78 (s, 1H, $H_{10}$), 8.31 (t, $J$ = 7.8, 1H, $H_5$), 8.13 (dd, $J$ = 8.4, $J$ = 7.2, 1H, $H_8$), 8.05 (s, 1H, $H_2$), 7.97 (dd, $J$ = 8.0, $J$ = 1.2, 1H, $H_6$), 7.87 (dd, $J$ = 7.6, $J$ = 0.8, 1H, $H_4$), 7.62 (d, $J$ = 8.4, 1H, $H_7$), 7.48 (m, 1H, $H_9$), 4.12 (m, 4H, NC$H_2$), 3.66 (s, 3H, $H_1$), 2.08 (m, 4H) (see Supporting Information for the numbering of the protons); MALDI-TOF (dithranol): calculated for $[C_{19}H_{20}F_3HgN_6O_3S]^+$ 671.0976, found 670.9325.

**4.8. Hg.1.N$_2$C$_5$.** The reaction mixture was heated at 60 °C. Thermodynamic equilibrium was reached after 24 h. $^1$H NMR ($CDCl_3$*/$CD_3CN$ 52/48): 8.82 (s, 1H, $H_{10}$), 8.79 (s, 1H, $H_3$), 8.33 (t, $J$ = 7.6, 1H, $H_5$), 8.13 (dd, $J$ = 8.4, $J$ = 7.2, 1H, $H_8$), 8.05 (s, 1H, $H_2$), 7.99 (d, $J$ = 7.6, 1H, $H_6$), 7.87 (d, $J$ = 7.6, 1H, $H_4$), 7.62 (d, $J$ = 8.8, 1H, $H_7$), 7.48 (m, 1H, $H_9$), 4.21 (m, 4H, NC$H_2$), 3.66 (s, 3H, $H_1$), 2.10−1.85 (m, 6H) (see Supporting Information for the numbering of the protons); MALDI-TOF (dithranol): calculated for $[C_{20}H_{22}F_3HgN_6O_3S]^+$ 685.1132, found 685.0686.

**4.9. Pb.1.N$_2$C$_3$.** Thermodynamic equilibrium was reached after 5 days at 60 °C. $^1$H NMR ($CDCl_3$*/$CD_3CN$ 56/44): 9.59 (d, $J$ = 2.0, 1H), 9.51 (d, $J$ = 2.0, 1H), 8.42−8.38 (m, 2H), 8.20 (dd, $J$ = 8.8, $J$ = 7.2, 1H), 8.07 (d, $J$ = 7.2, 1H), 7.96 (d, $J$ = 7.6, 1H), 7.61 (d, $J$ = 8.8, 1H), 7.54 (d, $J$ = 7.2, 1H), 4.43−4.28 (m, 4H, NC$H_2$), 3.72 (s, 3H, NC$H_3$), 2.47−2.43 (m, 2H, NCH$_2$C$H_2$); MALDI-TOF (dithranol): calculated for $[C_{18}H_{18}F_3N_6O_3PbS]^+$ 663.088, found 662.959.

**4.10. Pb.1.N$_2$C$_4$.** Thermodynamic equilibrium was reached after a few days at 60 °C. $^1$H NMR ($CDCl_3$*/$CD_3CN$ 56/44): 9.27 (s, 1H), 9.22 (s, 1H), 8.42 (s, 1H), 8.33 (t, $J$ = 7.8, 1H), 8.15 (dd, $J$ = 8.4, $J$ = 7.2, 1H), 8.00 (d, $J$ = 7.6, 1H), 7.91 (d, $J$ = 7.6, 1H),

(99) For systems chemistry, see for instance:(a) Stankiewicz, J.; Eckhardt, L. H. *Angew. Chem. In. Ed.* **2006**, *45*, 342–344. (b) Ludlow, R. F.; Otto, S. *Chem. Soc. Rev.* **2008**, *37*, 101–108.

(100) Gottlieb, H. E.; Kotlyar, V.; Nudelman, A. *J. Org. Chem.* **1997**, *62*, 7512–7515.

7.53 (d, $J = 8.8$, 1H), 7.50 (d, $J = 7.6$, 1H), 4.06 (m, 4H), 3.73 (s, 3H, NC$H_3$), 2.21 (m, 4H); MALDI-TOF (dithranol): calculated for $[C_{19}H_{20}F_3N_6O_3PbS]^+$ 677.1036, found 676.9883.

**4.11. Pb.1.$N_2C_5$.** Thermodynamic equilibrium was reached after 12−24 h when the sample was left standing without stirring. $^1$H NMR ($CDCl_3$*/$CD_3CN$ 59/41): 9.00 (m, 2H), 8.42 (s, 1H), 8.27 (t, $J = 7.8$, 1H), 8.10 (dd, $J = 8.4$, $J = 7.2$, 1H), 7.94 (dd, $J = 8.0$, $J = 1.2$, 1H), 7.85 (dd, $J = 7.6$, $J = 0.8$, 1H), 7.46 (m, 2H), 3.97 (m, 4H), 3.72 (s, 3H, C$H_3$), 1.97 (m, 6H); MALDI-TOF (dithranol): calculated for $[C_{20}H_{22}F_3N_6O_3PbS]^+$ 691.1193, found 691.0742.

**4.12. Pb.1.$N_2$O.** Thermodynamic equilibrium was reached after 12−24 h when the sample was left standing without stirring. $^1$H NMR ($CDCl_3$*/$CD_3CN$ 56/44): 9.05 (s, 1H), 9.02 (s, 1H), 8.26 (s, 1H), 8.21 (t, $J = 7.8$, 1H), 8.05 (dd, $J = 8.4$, $J = 7.6$, 1H), 7.86 (dd, $J = 7.6$, $J = 0.8$, 1H), 7.80 (dd, $J = 7.6$, $J = 0.8$, 1H), 7.42 (s, 1H), 7.40 (d, $J = 1.6$, 1H), 4.05−4.02 (m, 4H), 3.94−3.90 (m, 4H), 3.69 (s, 3H, NC$H_3$); MALDI-TOF (dithranol): calculated for $[C_{19}H_{20}F_3N_6O_4PbS]^+$ 693.098, found 692.984.

**4.13. Hg.1.$N_2$O.** Thermodynamic equilibrium was reached after 2 days. $^1$H NMR ($CDCl_3$*/$CD_3CN$: 52/48): 8.84 (br, 2H, C$H$N), 8.32 (t, $J = 7.6$, 1H, $H_5$), 8.12 (dd, $J = 8.8$, $J = 7.2$, 1H, $H_8$), 8.05 (s, 1H, $H_2$), 7.98 (d, $J = 8.0$, 1H, $H_6$), 7.89 (d, $J = 7.2$, 1H, $H_4$), 7.61 (d, $J = 8.8$, 1H, $H_7$), 7.48 (m, 1H, $H_9$), 4.26 (m, 4H, NC$H_2$), 4.06 (t, $J = 5.4$, 2H), 3.97 (t, $J = 5.4$, 2H), 3.65 (s, 3H, $H_1$); MALDI-TOF (dithranol): calculated for $[C_{19}H_{20}F_3HgN_6O_4S]^+$ 687.0925, found 686.8912.

**4.14. Pb.1.$N_2$NH.** Thermodynamic equilibrium was reached after 12−24 h when the sample was left standing without stirring. $^1$H NMR ($CDCl_3$*/$CD_3CN$ 56/44): 9.02 (s, 1H, $H_3$), 8.96 (s, 1H, $H_{10}$), 8.14 (t, $J = 7.6$, 1H, $H_5$), 8.08 (br, 1H, $H_2$), 7.99 (dd, $J = 8.8$, $J = 7.2$, 1H, $H_8$), 7.76 (d, $J = 8.0$, 1H, $H_6$), 7.71 (d, $J = 7.6$, 1H, $H_4$), 7.34 (m, 2H, $H_7 + H_9$), 4.02 (m, 4H, NC$H_2$), 3.65 (s, 3H, $H_1$), 3.28 (m, 4H, C$H_2$NH), 2.75 (m, 1H, $CH_2$N$H$) (see Supporting Information for the numbering of the protons); MALDI-TOF (dithranol): calculated for $[C_{19}H_{21}F_3N_7O_3PbS]^+$ 692.1145, found 692.1012.

**4.15. Zn.1.$N_2$NH.** The reaction mixture was heated at 65 °C. Thermodynamic equilibrium was reached after 24 h. $^1$H NMR ($CDCl_3$*/$CD_3CN$ 6/4): 8.58 (s, 1H), 8.07 (m, 2H), 7.95 (m, 2H), 7.63 (d, $J = 7.2$, 1H), 7.43 (m, 2H), 5.19 (br, 1H), 4.05−2.74 (m, 8H), 3.65 (s, 3H, NC$H_3$); MALDI-TOF (dithranol): calculated for $[C_{19}H_{21}F_3N_7O_3SZn]^+$ 548.067, found 547.951.

**4.16. General Procedure for the Competition Experiments between Two Different Diamines.** The two diamines (3 $\mu$mol of each in 50 $\mu$L of $CDCl_3$/$CD_3CN$ 6/4) were placed in an NMR tube. The dialdehyde **1** (3 $\mu$mol in 0.6 mL of $CDCl_3$/$CD_3CN$ 6/4) was added. The metal salt (3 $\mu$mol) was then added from a 60 mM $CDCl_3$/$CD_3CN$ 6/4 solution in the case of zinc triflate, 30 mM $CD_3CN$ solution in the case of mercury triflate, and 60 mM $CD_3CN$ solution in the case of lead triflate.

**Acknowledgment.** We thank Drs. Augustin Madalan and Lydia Brelot for X-ray diffraction analyses and Romain Carrière for MALDI-TOF mass spectrometry analyses. Sébastien Ulrich thanks the French Ministère de la Recherche for a doctoral fellowship.

**Supporting Information Available:** Complementary data such as mass spectrometry results, 2D NMR and $^1$H NMR competition experiment results. This material is available free of charge via the Internet at http://pubs.acs.org.

JA809828G